

Institute of High Energy Physics
Chinese Academy of Sciences

SiPMs

IHEP, Beijing 2018

Véronique PUILL

CNRS IN2P3 Les deux infinis
LABORATOIRE DE L'ACCÉLÉRATEUR LINÉAIRE
Faculté des sciences d'Orsay

Outline

- The photodetection process in Silicon devices
- The main Si detector characteristics
- From the PIN photodiode to the SiPM
- Caracteristics of SiPM

Basic principle of the Photodetection

Goal of the Photodetection: convert Photons into a detectable electrical signal

The transformation of light into an electrical signal in a photodetector follows 3 steps : the photoconversion, the photo-electron collection and the signal multiplication

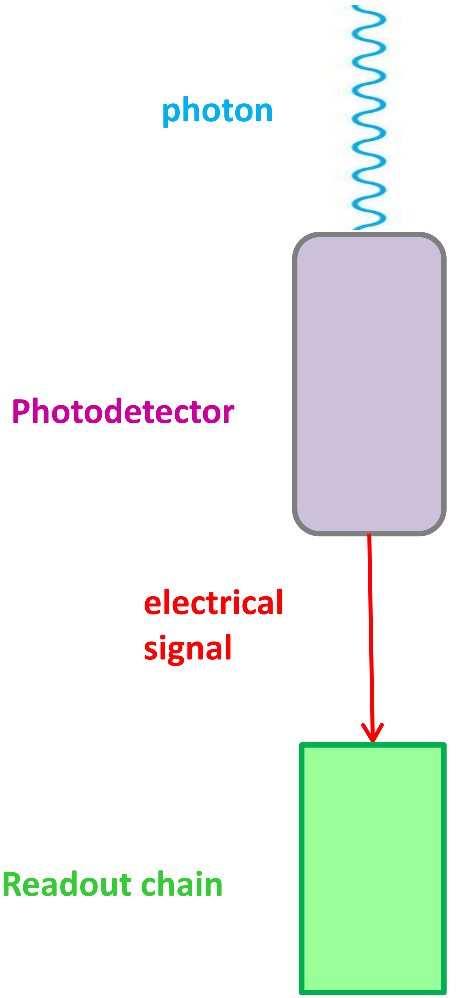

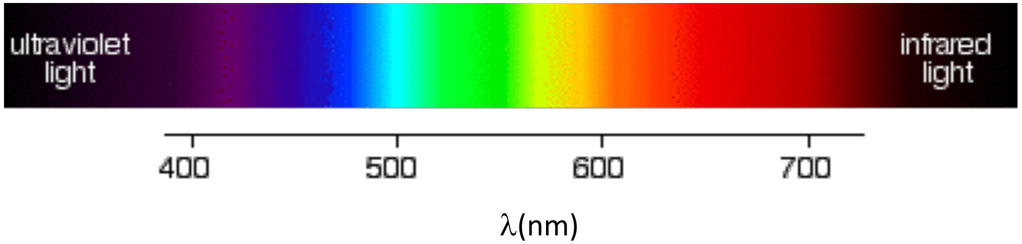

1. Photoconversion: photoelectric effect

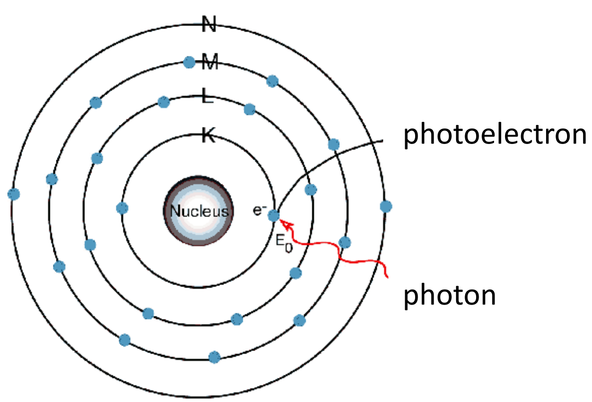

2. Photo-electron collection

3. Signal multiplication

Phase 1 : the Photoconversion in Si

Photons entering a silicon layer travel a characteristic distance (absorption length)

The light is absorbed in the Si according to the Beer-Lambert law

$$I(\lambda,z) = I(\lambda)e^{-\alpha(\lambda)z}$$

I(λ) : initial photon flux
I(λ,z) : photon flux on the distance z from SiPM surface
α(λ): optical absorption coefficient
z : penetrated thickness in Si

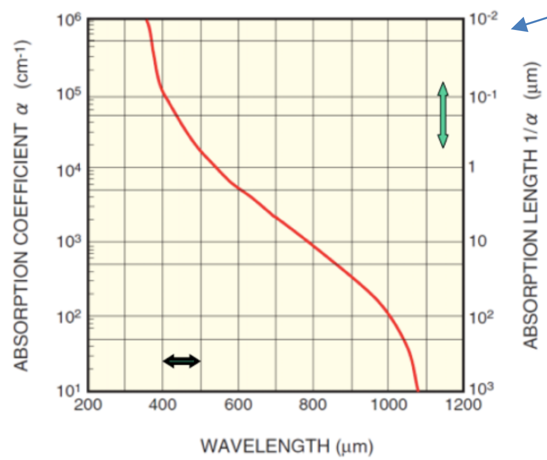

photons in the blue region are absorbed in the first µm of the detector whereas the red photons have to travel farther in the Si before being absorbed

Photon give up their energy to create a photoelectron (this energy has to be greater that the band gap energy), the e- is pulled up into the conduction band, leaving hole in its place in the valence band.
These e- and holes created are called the **carriers**.

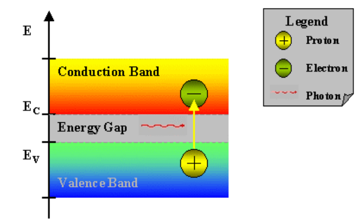

Band gap (T=300K) = 1.12 eV

→ for Si-photodetector this leads to a photocurrent: internal photoelectric effect

From photons to an electrical signal

Phase 2: the Photoelectron collection

Once the carriers are created they have to avoid absorption or recombination to be collected and give a signal at the output detector

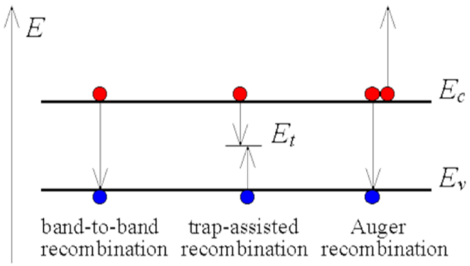

Need of a good **collection efficiency (C_E)**: probability to transfer the primary p.e or e/h to the readout channel or the amplification region

Phase 3: the signal multiplication

The primary electron/hole pair is amplified (photodetector with **internal gain**)

Some photodetectors incorporate internal gain mechanisms so that the photoelectron current can be physically amplified within the detector and thus make the signal more easily detectable.

The main Si detector characteristics

- Sensitivity
- Noise
- Gain
- Linearity
- Time response

Sensitivity

The efficiency of the conversion process is measured by the **quantum efficiency** (probability that the incident photon (Nγ) generates a photoelectron (Npe) that contributes to the detector current)

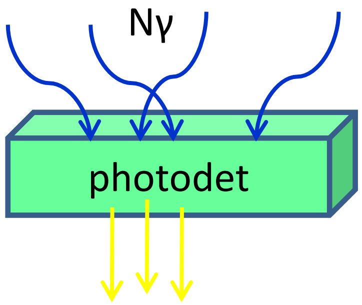

Sensitivity x Gain x Npe

Quantum efficiency

$$Q\varepsilon[\%] = \frac{N_{pe}}{N_{\gamma}}$$

Radiant sensitivity

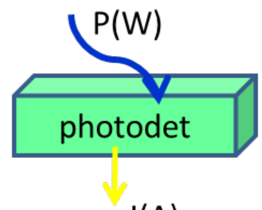

$$S[mA/W] \approx \frac{Q\varepsilon[\%] x \lambda[nm] x qe}{hxc} = \frac{Q\varepsilon[\%] x \lambda[nm]}{124}$$

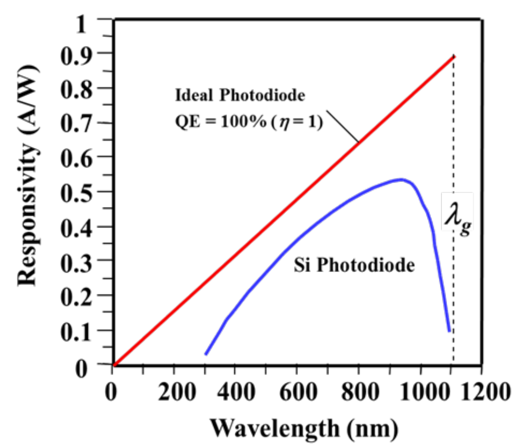

Photo detection efficiency (SiPM)

In the SiPM case, the sensitivity is given by the PDE which combines the Qε and 2 other factors : *Ɛgeom:* geometrical factor and Ptrig: triggering probability

$$PDE\ [\%] = \mathcal{E}geom\ [\%] \times Q\varepsilon[\%] \times Ptrig\ [\%]$$

Gain and its fluctuations

In high electric field (≈ 10^5 V · cm^{-1}) the carriers are accelerated and can rich an energy higher than the ionization energy of valent electrons →this process called impact ionisation leads to the carriers multiplication

Gain (G): charge of the pulse when one photon is detected divided by the electron charge

$$G = \frac{Q_{signal}}{q_e}$$

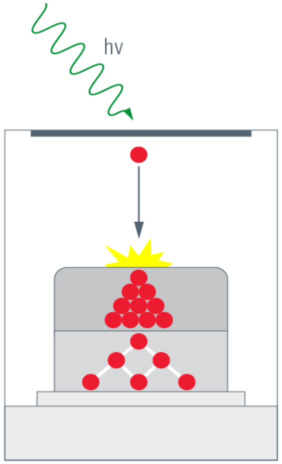

The photodetector output current fluctuates.
The noise in this signal arises from 2 sources:

- randomness in the photon arrivals
- randomness in the carrier multiplication process

The statistical fluctuation of the avalanche multiplication which widen the response of a photodetector to a given photon signal beyond what would be expected from simple photoelectron statistics (Poisson) is characterized by the **excess noise factor ENF**

$$ENF = 1 + \frac{\sigma_G^2}{G^2}$$

ENF

- impacts the photon counting capability for low light measurements
- deteriorates the stochastic term in the energy resolution of a calorimeter

Photodetector noise

Noise is a general term that covers all sources of unwanted signal that are superimposed to the pulse we are interesting in and imposes a limit on the smallest signal that can be measured.

Principal noises associated with photodetectors :

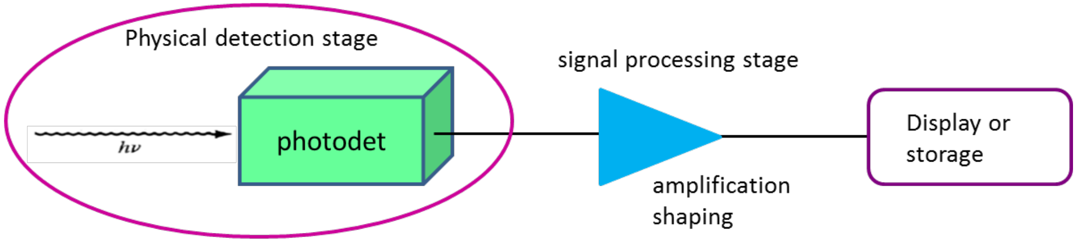

Shot noise:

statistical nature of the production and collection of photo-generated electrons upon optical illumination (the statistics follows a Poisson process)

Dark current noise:

the current that continues to flow through the bias circuit in the absence of the light :

- **bulk dark current** due to thermally generated charges
- **surface dark current** due to surface defects

The dark noise depends a lot on the threshold → not a big issue when we want to detect hundreds or thousands of photons but crucial in the case of very weak incident flux ....

Linearity

Ideally, the photocurrent response of the photodetector is linear with incident radiation over a wide range. Any variation in responsivity with incident radiation represents a variation in the linearity of the detector

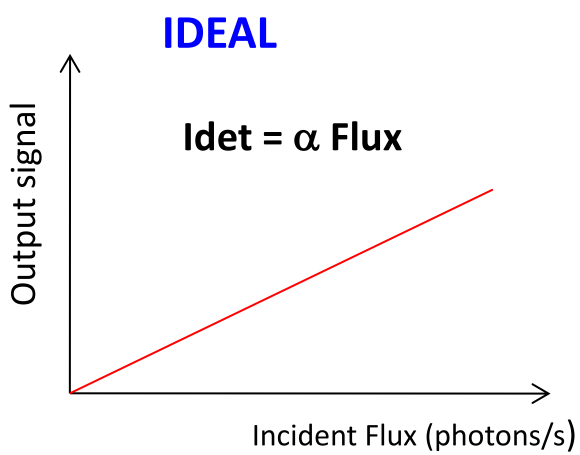

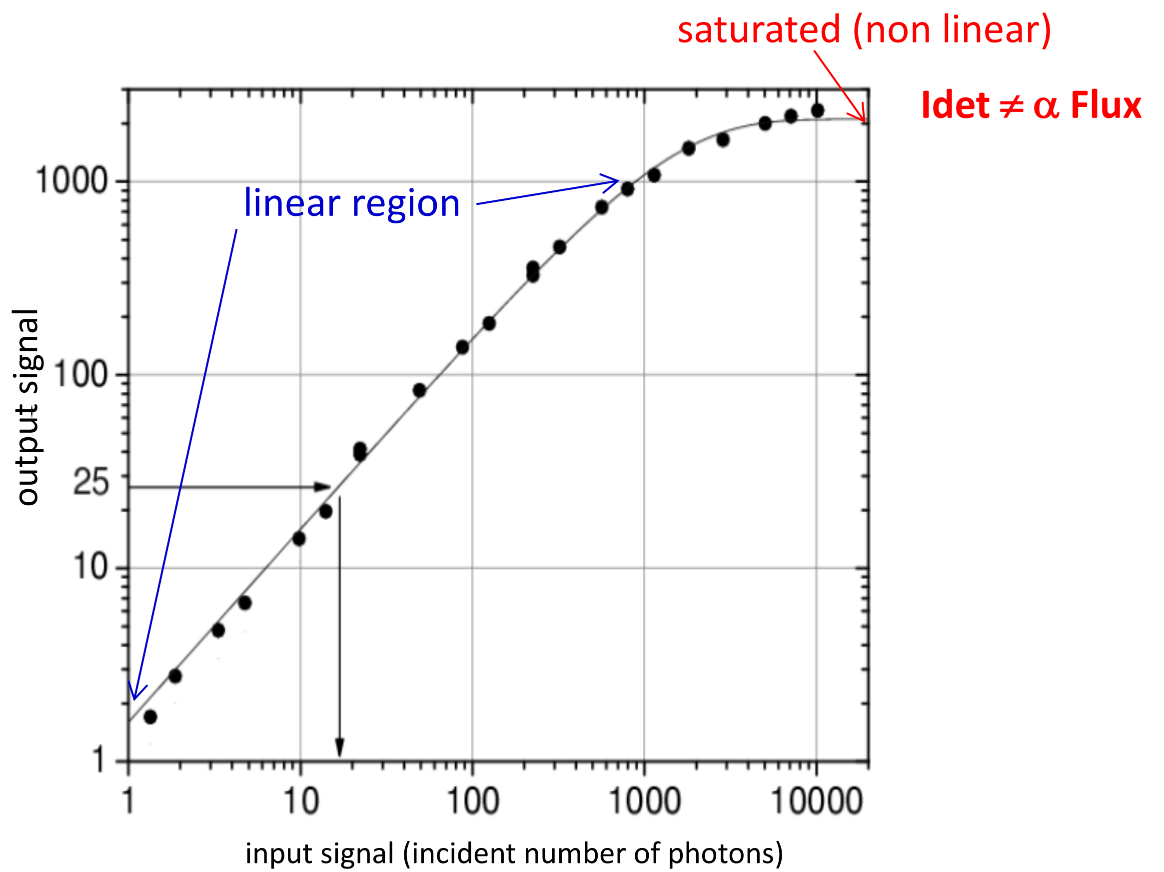

Saturation: issue for the measurement of large number of photons (calorimeter)

Time response

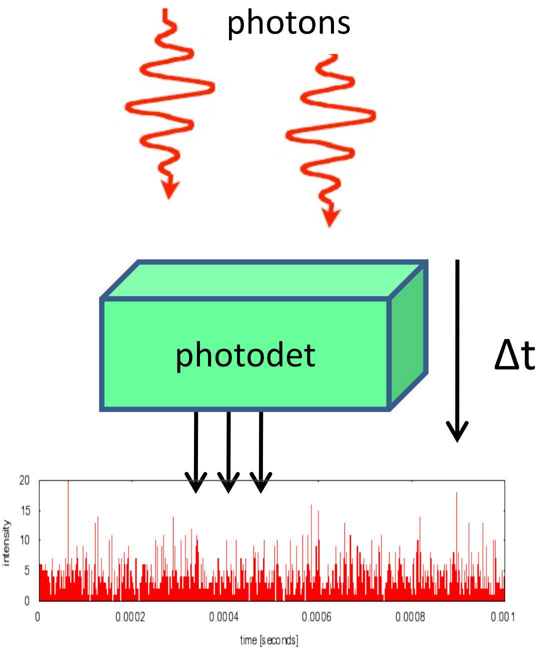

Electrical signal

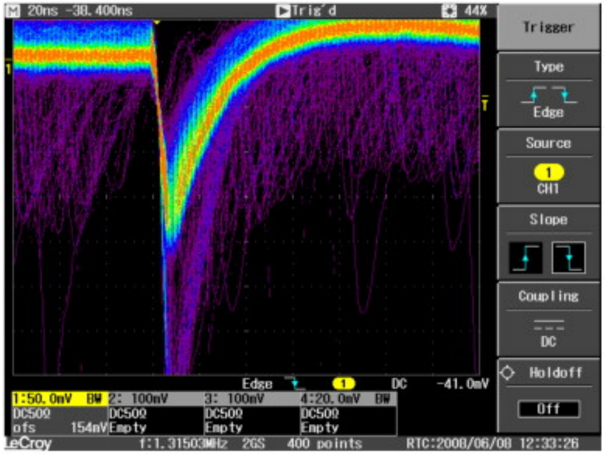

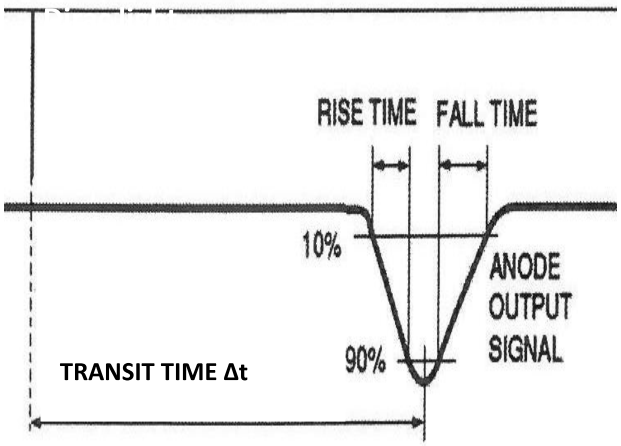

Timing parameters of the signal:

- Rise time, fall time (or decay time)
- Duration
- Transit time (Δt): time between the arrival of the photon and the electrical signal
- Transit time spread (TTS): transit time variation between different events

→ timing resolution

From the PIN photodiode to SiPM

The PIN photodiode

Schematic structure of an idealized PIN PD

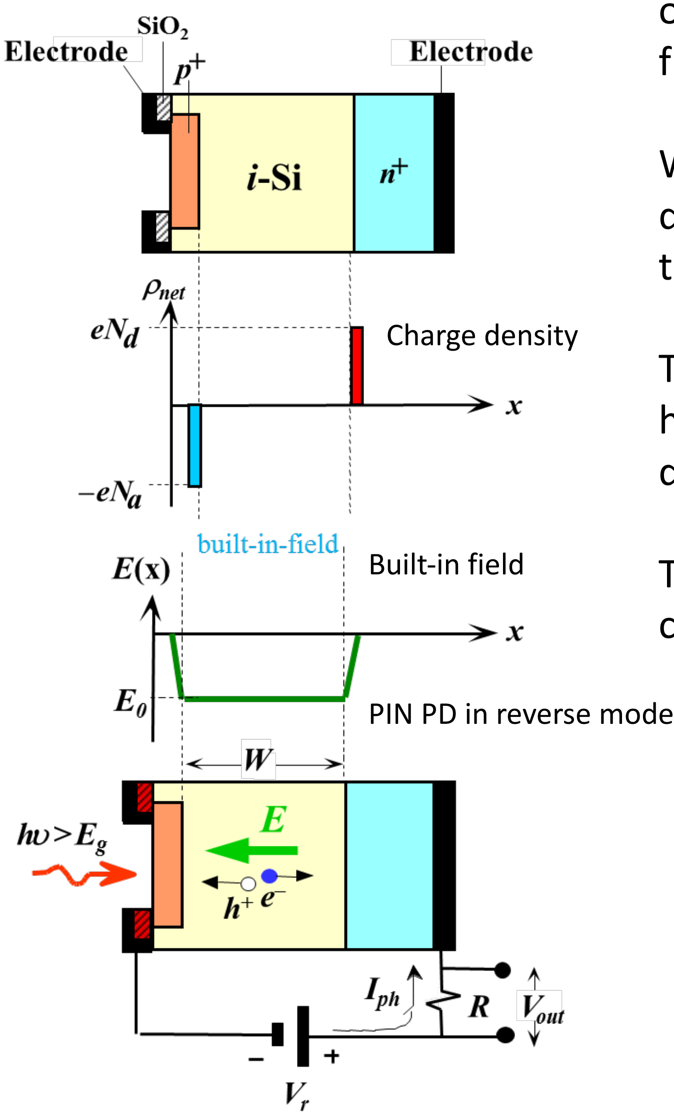

S.O Kasap, Optoelectronics, 1999

High purity Si with highly doped p+ and n+ type contacts on opposite surfaces. These 2 charges layers produce an electrical field

When light is incident on the p layer entrance window of the detector (which as to be transparent), it produces e-h pairs in the depletion layer (1 - 3 µm thick).

The internal electric field sweeps the e- to the n+ side and the hole to the p+ side → a drift current that flows in the reverse direction from the n+ side (cathode) to the p+ side (anode)

This transport process induces an electric current in the external circuit.

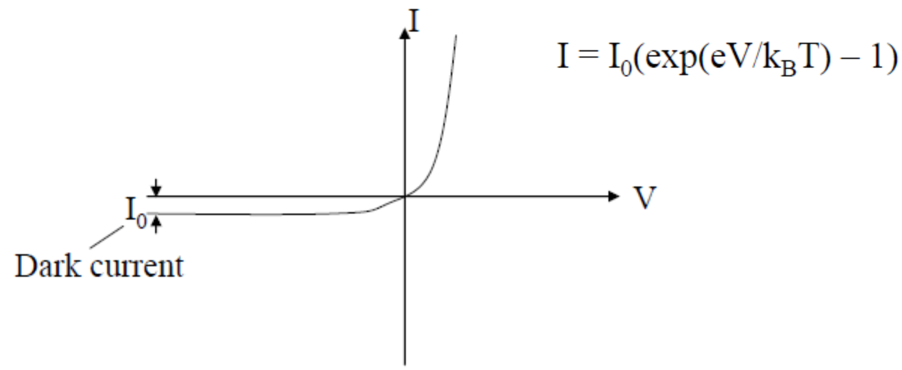

I_0 : thermal-generated free carriers which flow through the junction

The PIN photodiode

PIN photodiodes were the first large scale application of silicon sensors for low light level detection.

Their development was driven to find a replacement for photomultipliers in high HEP experiments, where detector elements had to be placed in magnetic fields.

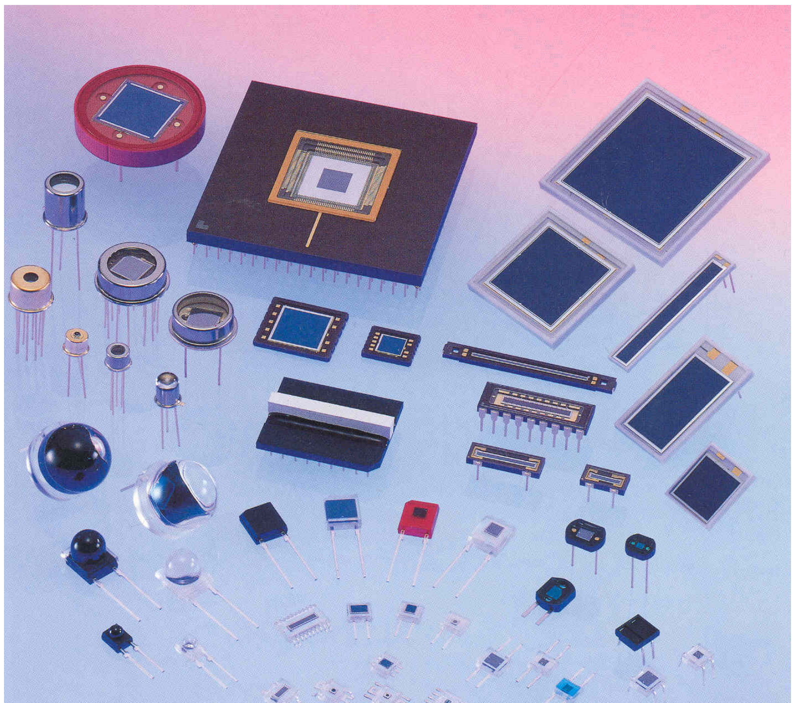

Example of PIN photodiode (Hamamatsu data sheet)

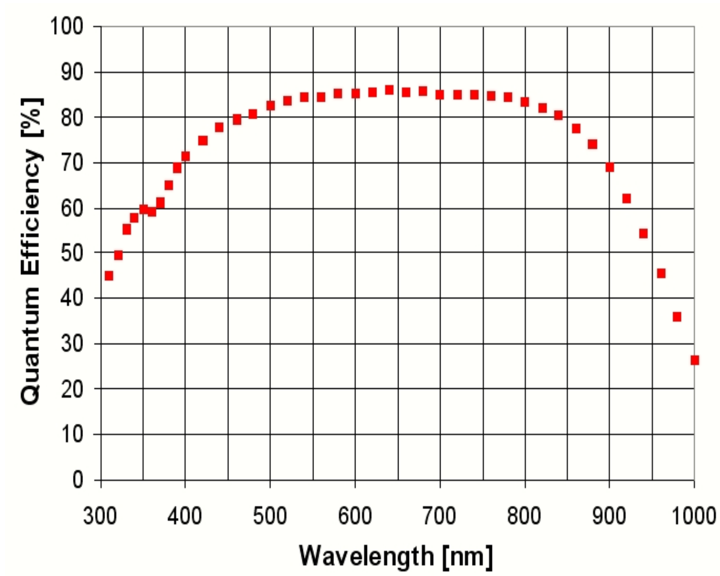

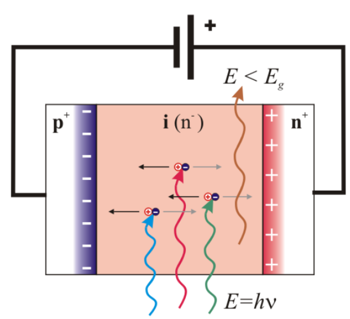

- high QE (80% @ 700nm)
- **But Gain = 1**

The Avalanche Photodiode

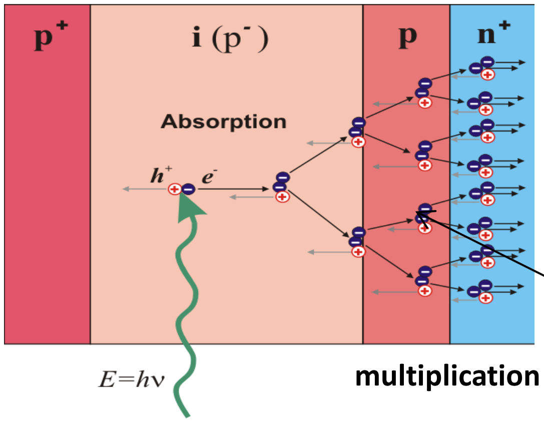

1. large reverse bias across the junction (50 - 200 V)

2. high electric field (≈ 10^5V/ cm) in the depletion region

3. the generated e- and holes may acquire sufficient energy to liberate more e- and holes within this layer by a process of impact ionization and these new carriers can initiate other pairs starting an avalanche.

Ionization coefficients α for electrons and β for holes

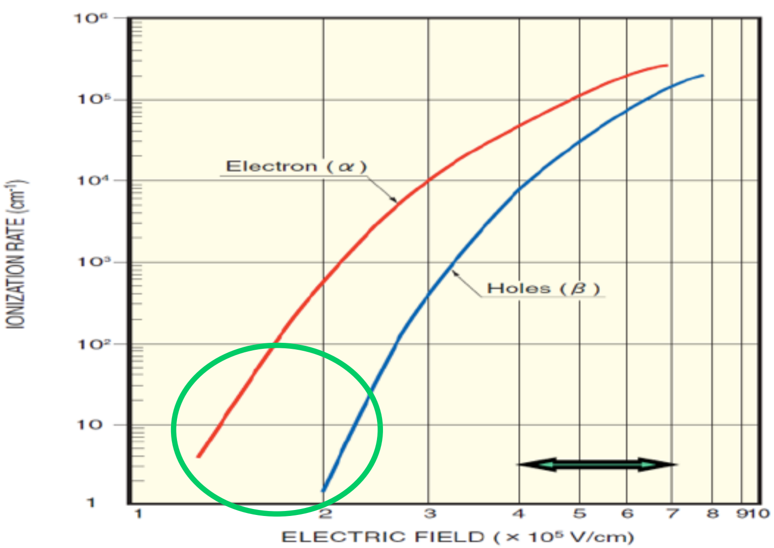

Ionization coffient for avalanche Multiplication

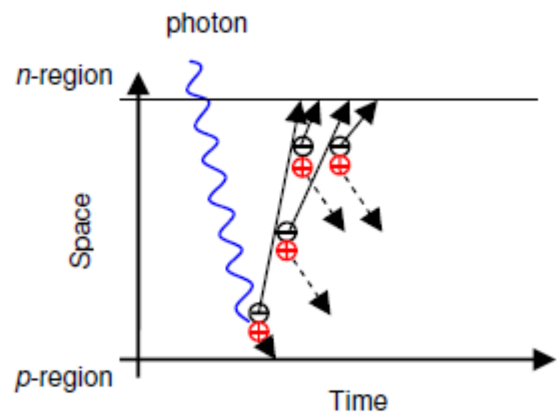

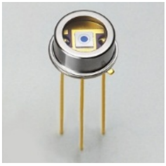

At this electric field (~10^5), the impact ionization coefficient of holes is much lower and the avalanche process is created practically only by electrons
→ avalanche process one directional and self quenched when carriers reach the border of depleted area.

The Avalanche Photodiode

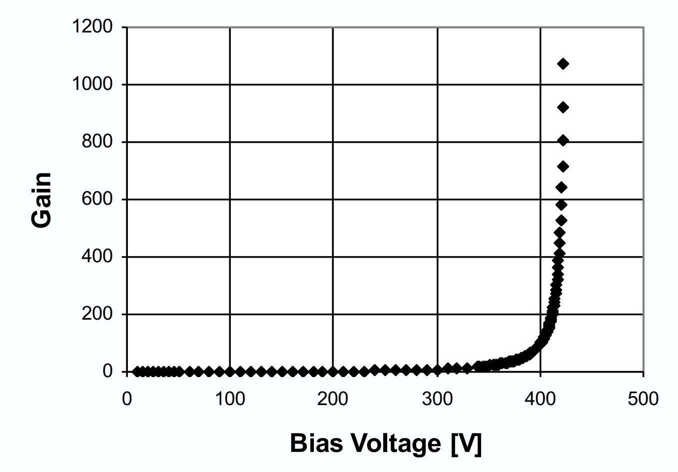

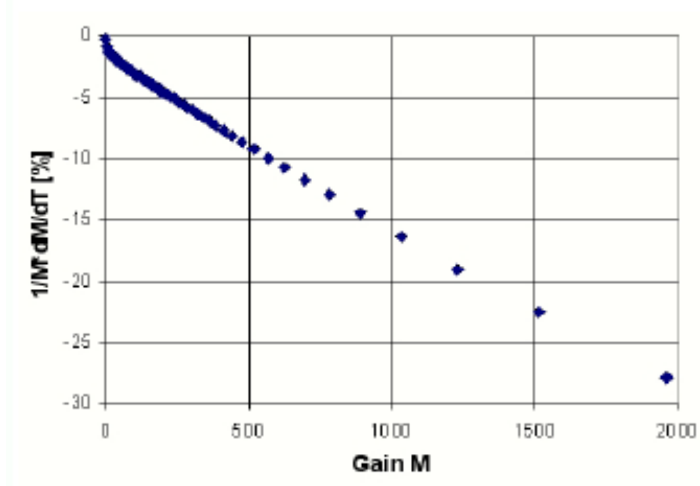

D. Renker, 2009 JINST 4 P04004

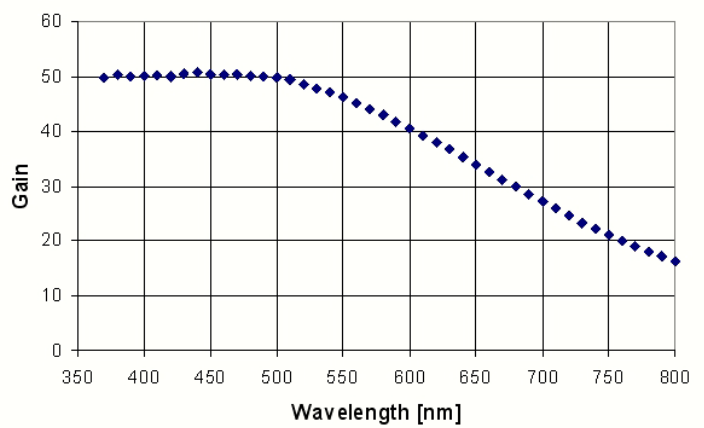

APDs (≈ 120000) in the ECAL of CMS

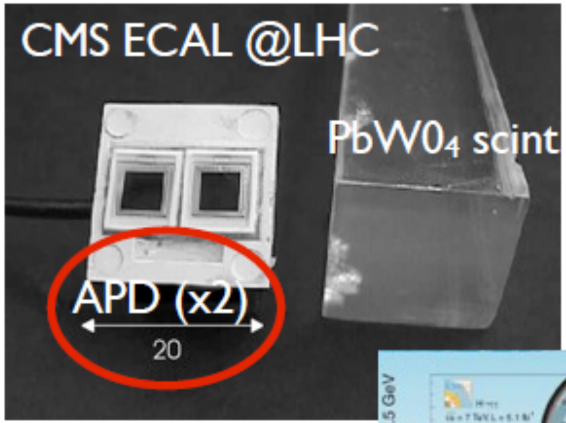

working gain ~ 50
Vbias ~70V

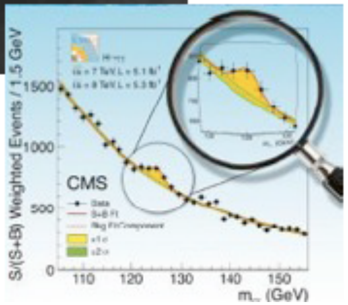

CMS APDs (bias voltage : 50 – 200 V)

- high QE (80% @ 500nm)
- Gain = 50 – 100
- high variation with temp. and bias voltage : ΔG = 3.1%/V and -2.4 %/°C (gain= 50)

From PIN photodiode to Geiger mode APD

Geiger mode -APD

- $V_{bias} > V_{BD}$
- G ⇨ ∞
- single photon level

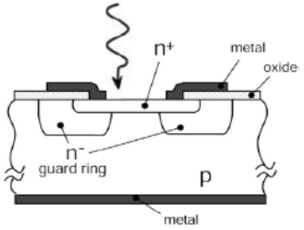

R.H. Haitz.,, J. Appl. Phys. 35 (1964)

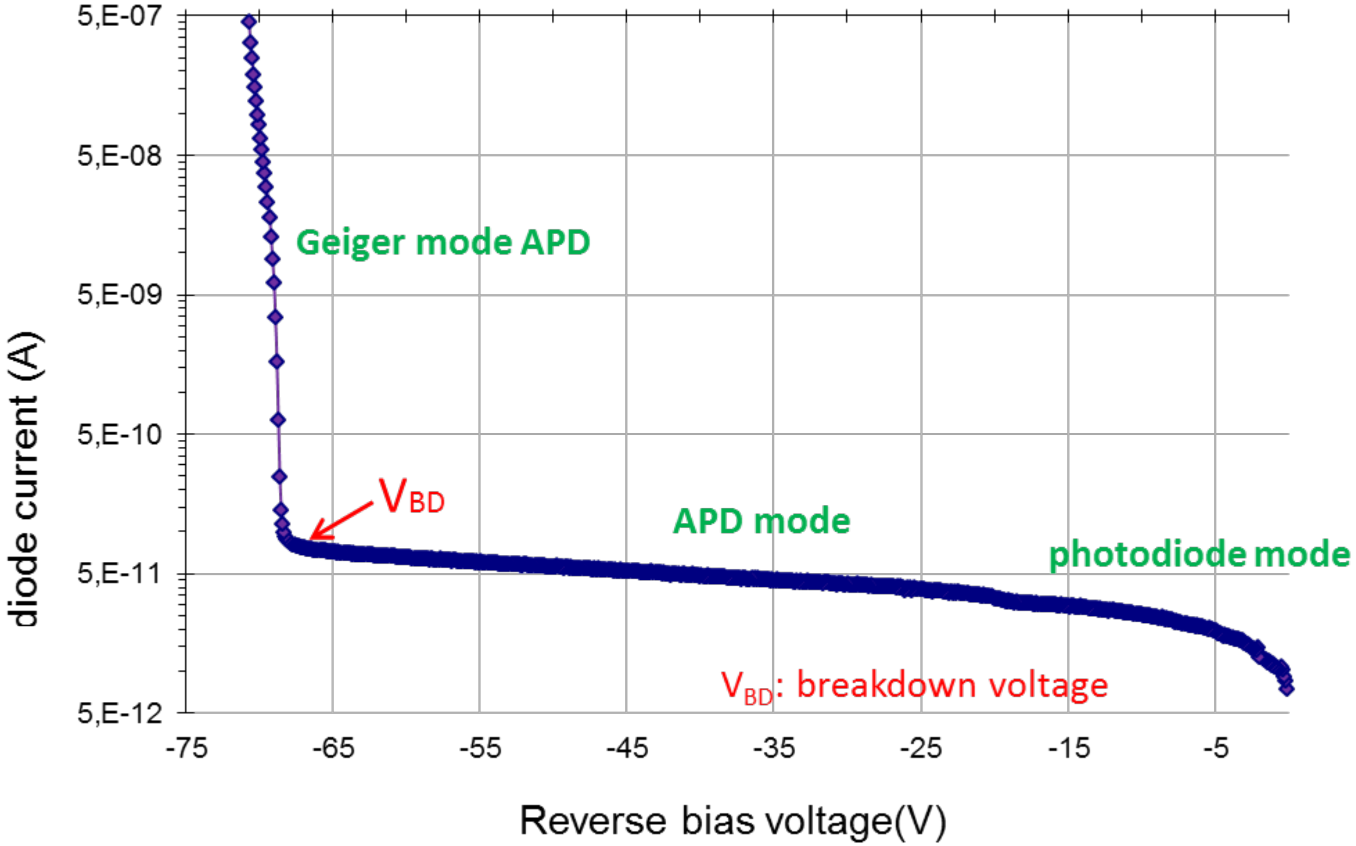

APD

- $V_{APD} < V_{bias} < V_{BD}$
- G = M (50 - 100)
- Linear-mode operation

Photodiode

- $0 < V_{bias} < V_{APD}$ (few volts)
- G = 1
- Operate at high light level (few hundreds of photons)

The Geiger mode APD

Valeri Saveliev, ISBN 978-953-7619-76-3

Schematic structure of a G-M APD

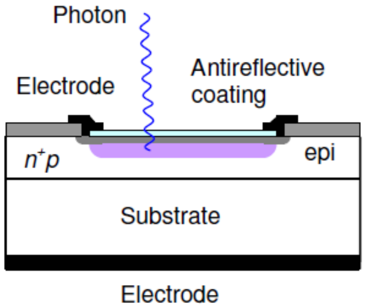

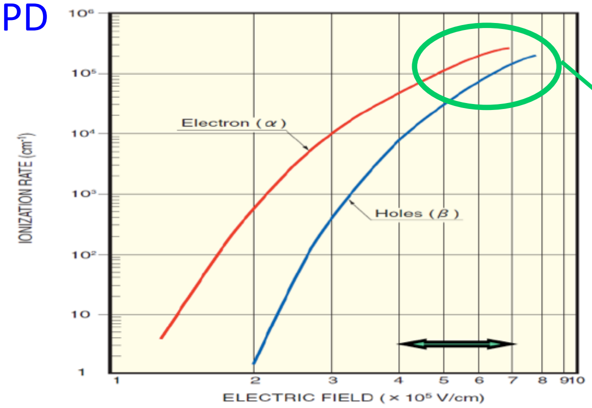

Ionization coffient for avalanche Multiplication

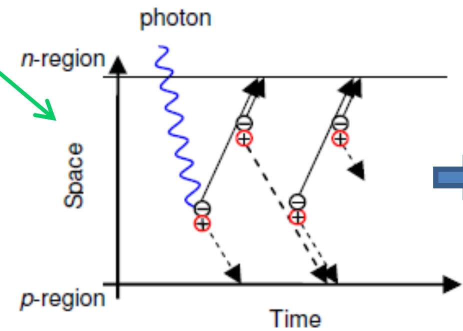

➡ breakdown

equivalent electrical circuit

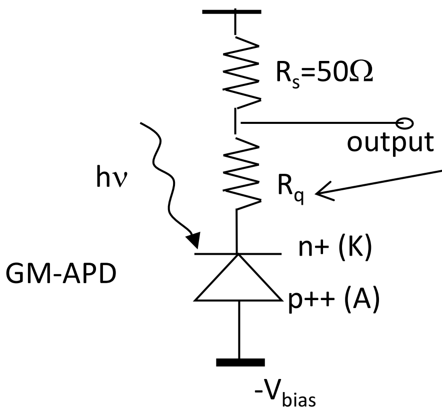

both type of carriers participate in the avalanche process → creation of a self-sustaining avalanche → current rises exponentially with time and reach the breakdown condition. No internal "turn-off" → the avalanche process must be quenched by the voltage drop across a serial resistor : quenching resistor

G = 10^5-10^6

G-M APD output signal

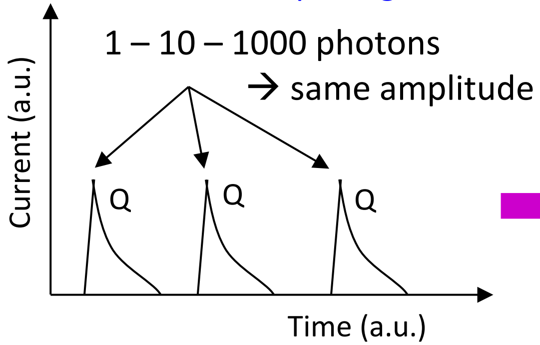

➡ Binary device : output signal (charge or amplitude) is not proportional to the number of incident photons

➡ No information of the light incident intensity with this kind of detector

Structure and principle of a SiPM

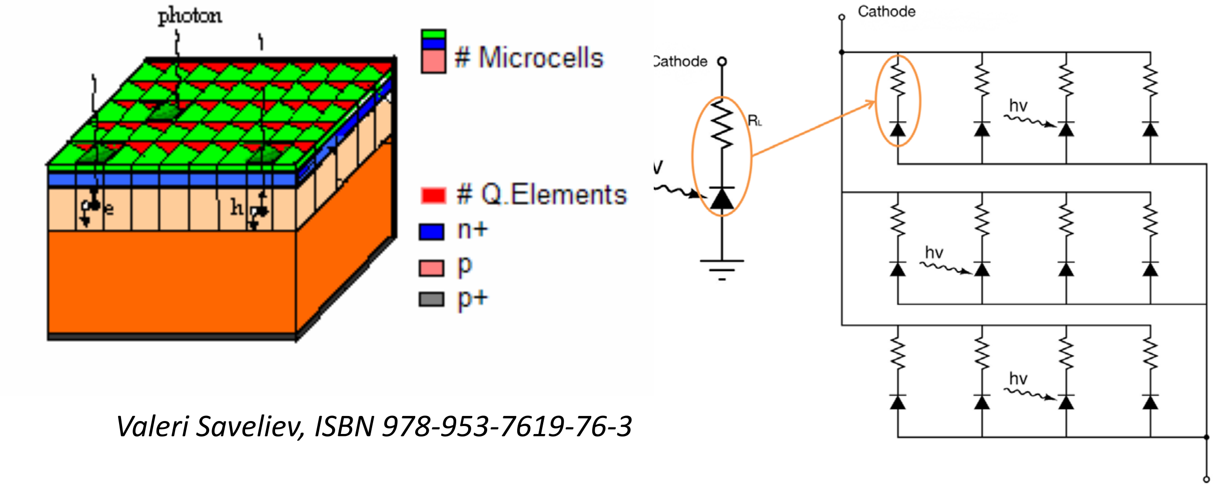

Valeri Saveliev, ISBN 978-953-7619-76-3

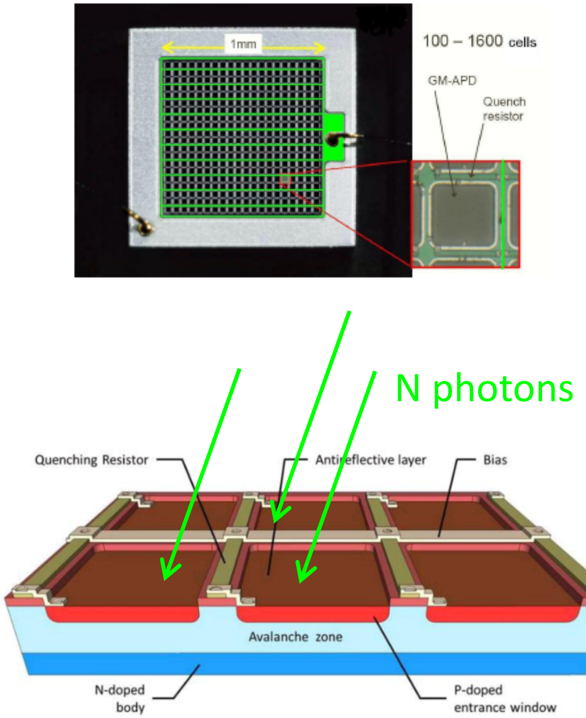

KETEK web site

- GM-APDs (cell) -few hundreds/mm²- connected in parallel
- Each cell is reverse biased above breakdown
- Self quenching of the Geiger breakdown by individual serial resistors

Each element is independent and gives the same signal when fired by a photon

⇓

output charge is proportional to the number of of incident photons

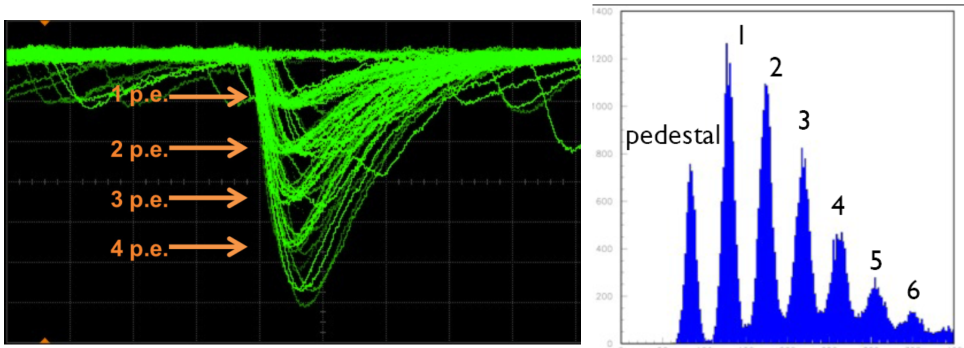

overlap display of pulse waveforms

G. Bisogni, RESMDD10

equivalent electrical circuit of a SiPM cell

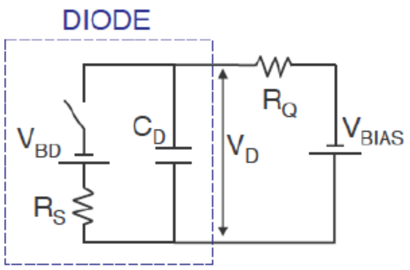

V_{BD} : breakdown voltage
R_Q : quenching resistance
R_S : Si substrate serie resistance (<< R_Q)
C_D : diode capacitance
V_{BIAS} : bias voltage

Vbias > Vbd

Fundamental operation modes in a GM-APD: quiescent mode, discharge, quenching and recovery phases

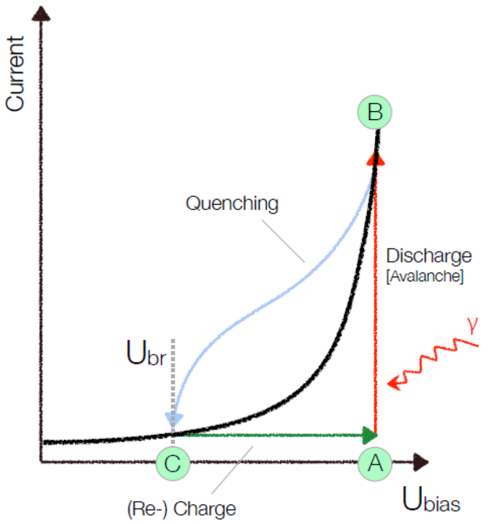

Quiescent mode
- Switch opened
- Unless a photon is absorbed or a dark event occurs, the current stay stable

Discharge phase
A → B : avalanche triggered, switch closed
C_D **discharges** to V_{BD} with the time constant $\tau = R_S \times C_D$ → during this phase, avalanche multiplication is ongoing inside the GM-APD → asymptotic grows of the current

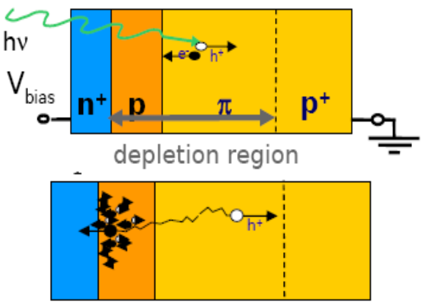

G.Collazuol, LIGHT11

Development of the signal in a cell

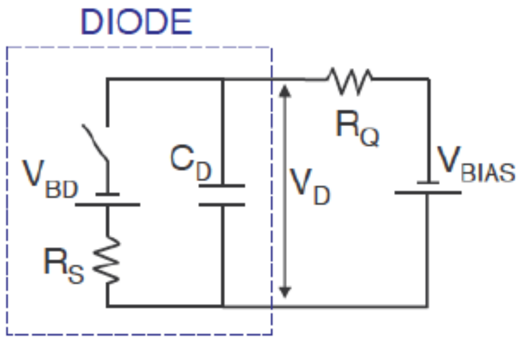

Quenching phase (B→ C)

- drop of the current across R_Q that leads to a reduction of the voltage in the diode → less and less charge carriers going through the multiplication regions → quenching of the photocurrent which prevent further Geiger-mode avalanche from occurring
- **avalanche quenched**
- switch open

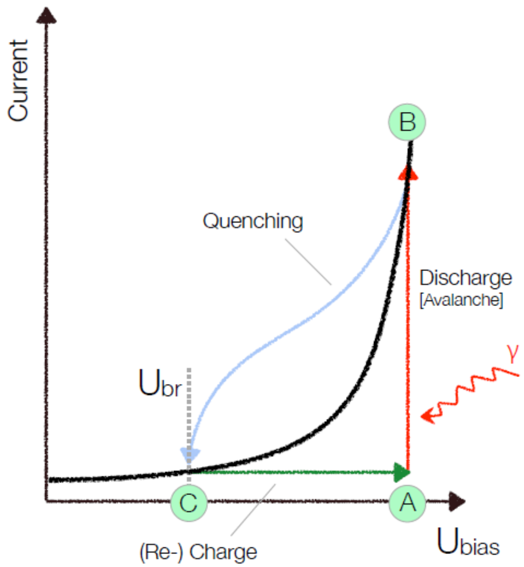

Recovery phase (C→ A) :

- C_D **recharges** through R_Q with the time constant $\tau' = R_Q \times C_D$
- **reset of the system**
- the GM-APD returns in the quiescent mode, ready for the detection of a new photon.

Characteristics of SiPM

Important photodetectors parameters

Photodetectors parameters

- Photon Detection Efficiency ●
- Dark noise rate ●
- Correlated noise ●
- Timing capability ●
- Signal shape ●
- Gain ●
- Radiation hardness ●
- Geometry ●
- Temperature dependence ●
- Packaging ●

System requirements

- ◆Large dynamic range (Calo, Astro, ..)
- ◆Timing Resolution (TOF PID, PET, …)
- ◆Energy resolution (Calo, PET, ..)
- ◆Large or complicated systems (HEP, Astro, medical appli, …)

Important photodetectors parameters

Photodetectors parameters **System requirements**

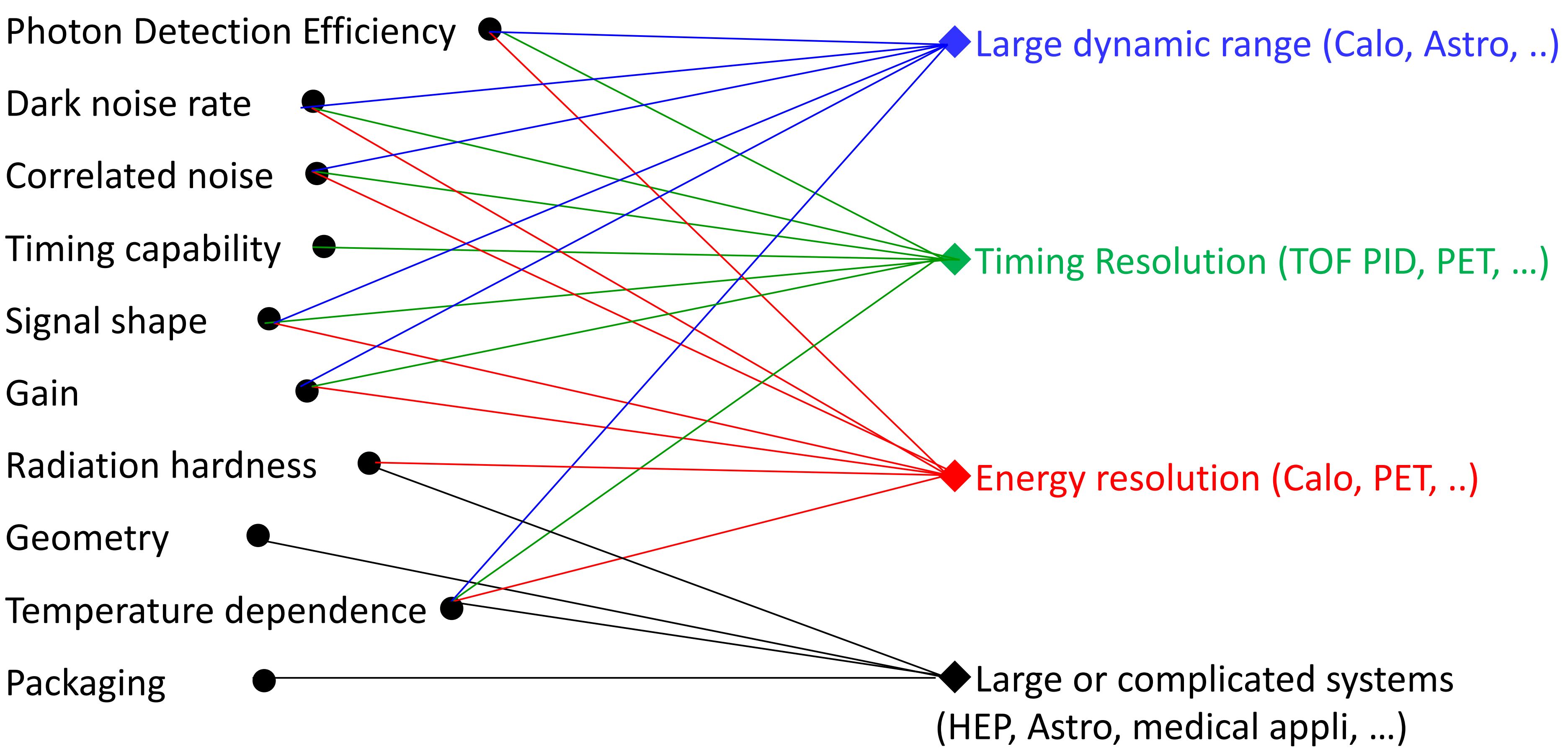

What does it look like?


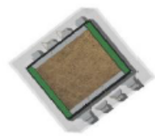
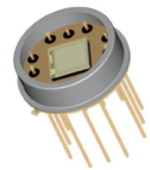
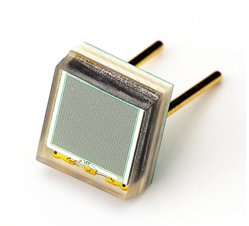
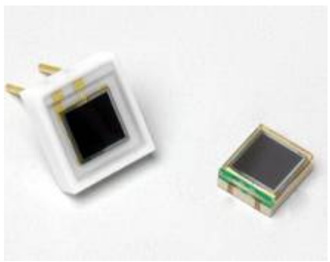

Dimensions: 1 mm² to 16 mm²

Cell size: 15 µm, 25, …, 100 µm

Matrixes: 4 to 256 channels

Packaging: metal (TO8), ceramic, plastic, with pins, surface mount type, matrix


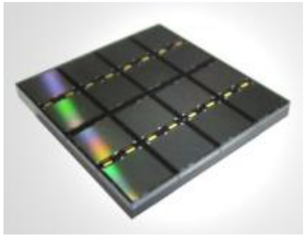
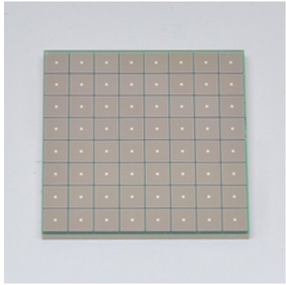

Who developp it ?

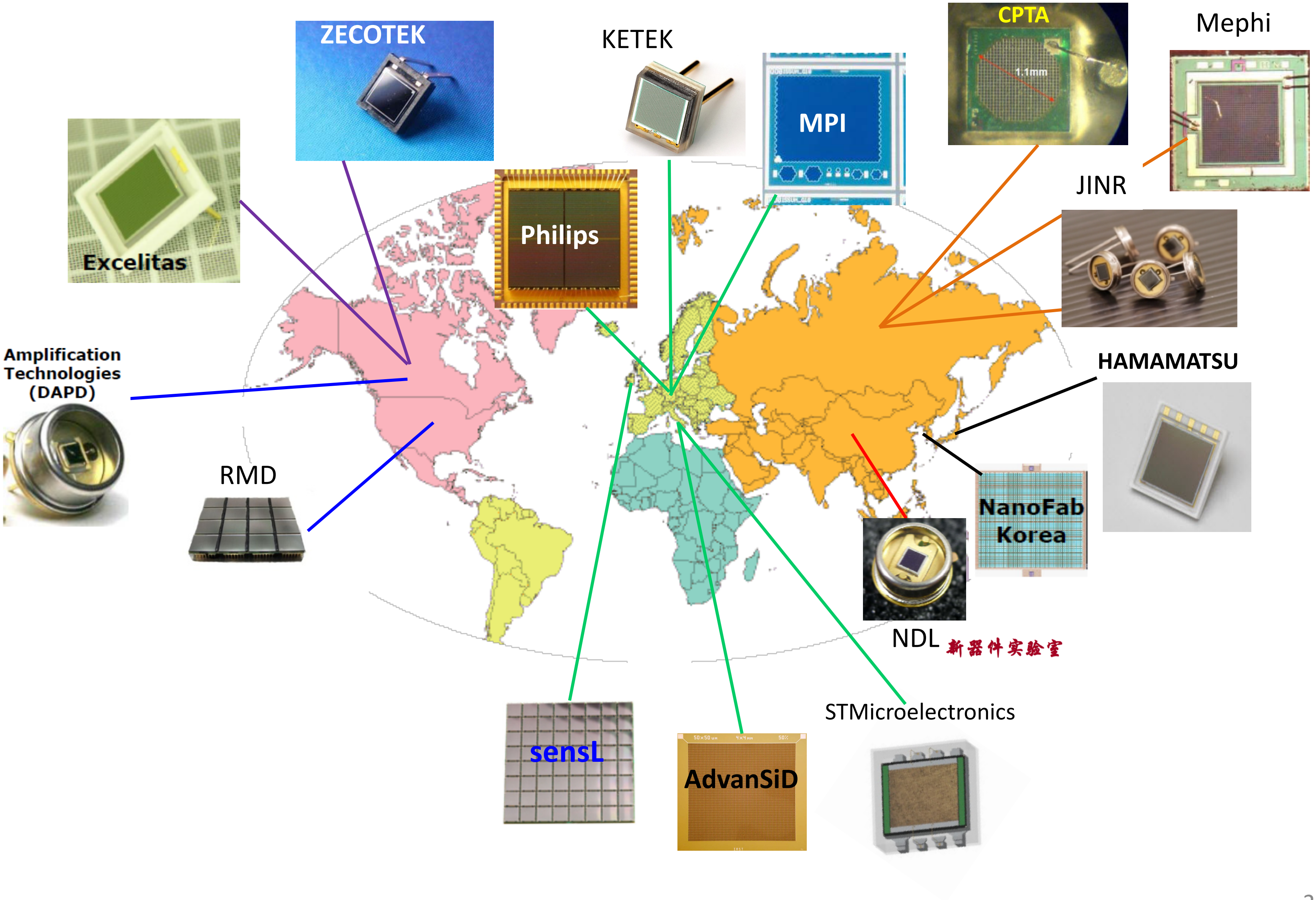

Signal pulse shape

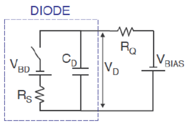

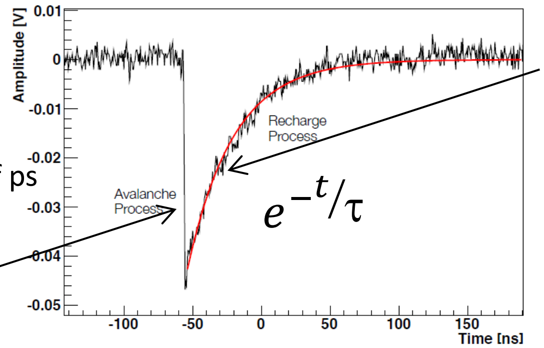

$$e^{-t/\tau}$$

Fast rise time: hundreds of ps

$T_R = R_S C_D$

$$1 - e^{-t/T_R}$$

Recovery time: tens to hundreds of ns

Time to recharge a cell after a breakdown : $\tau = R_Q C_D$

Different devices, diferent shapes

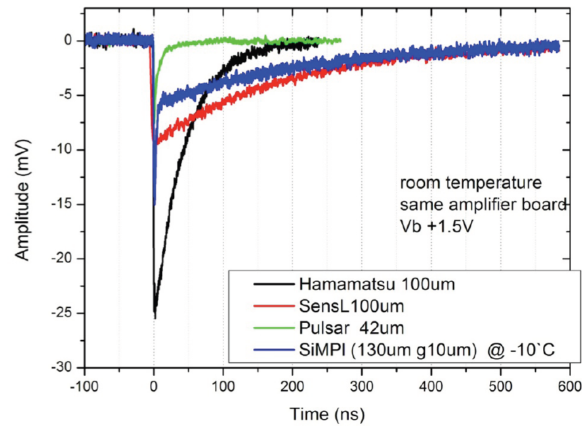

The rising edge corresponds to the discharge phase ($R_S C_D$) while the slower trailing edge is the recovery phase with time constant $R_Q C_D$

R_Q in Polysilicon

Poly-Si are temperature dependent: the resistor value increases as the temperature decreases →strong dependence of the recovery time with the temperature

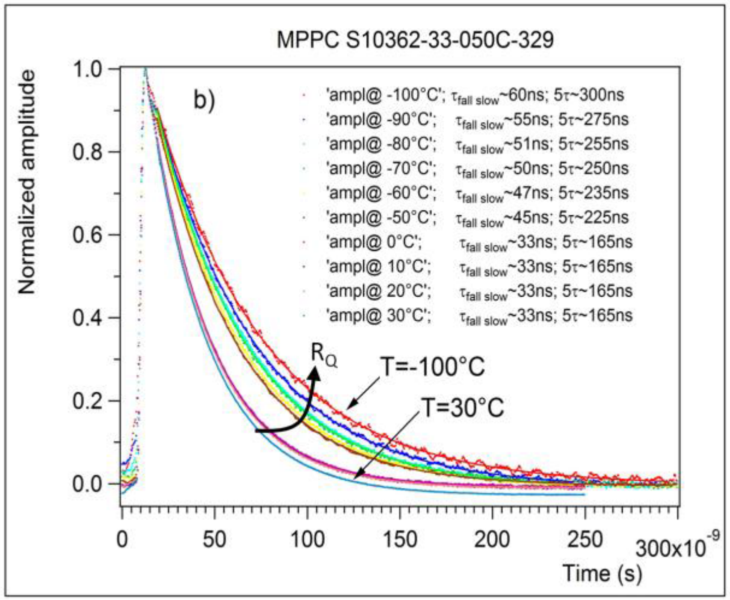

Dinu, IEEE NSS 2010

Metal Quenching Resistor (MQR)

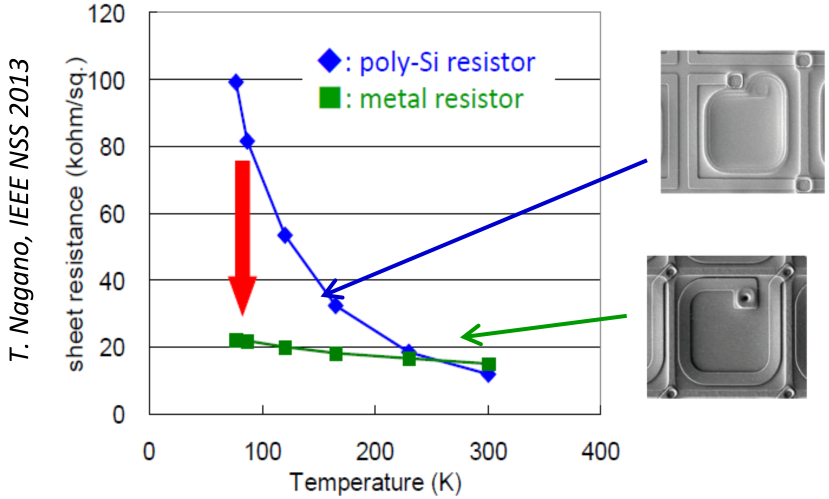

Good Uniformity of resistance
(full 6-inch wafer)

Width	Poly-Si	Metal
2 μm	19%	9%
1 μm	37%	11%

Low Temperature coefficient of resistance

Poly-Si	Metal
-2.37 kΩ	-0.43 kΩ

(/deg C)

The metal resistor has 1/5 lower temperature coefficient of resistance than poly-Si resistor

MQR with high transmittance → directly on the photosensitive surface → higher fill factor

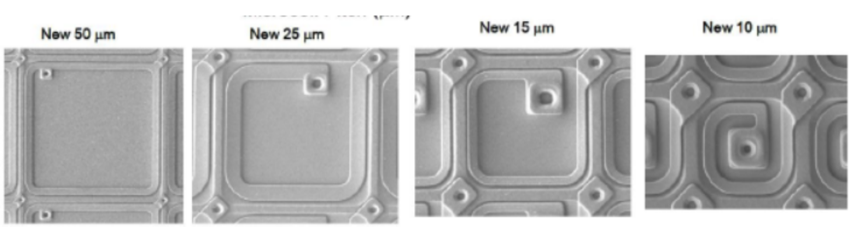

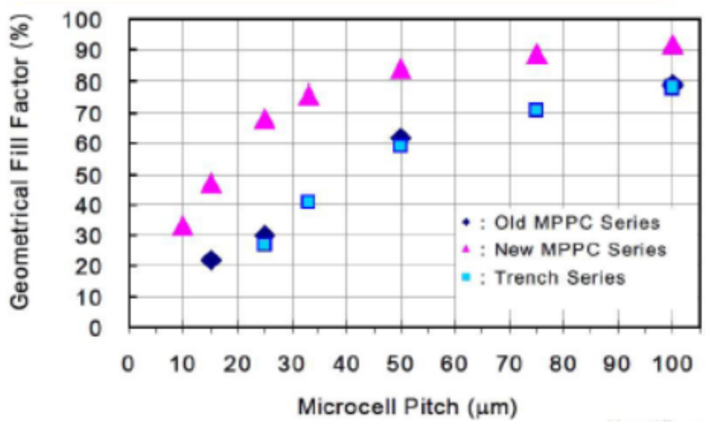

K. Yamamoto, 2nd SiPM Advanced Workshop, March 2014

Alternative quenching : bulk integrated resistor

Special design: both the matrix of avalanche regions and the individual quenching elements are created inside the Si substrate with a special distribution of the inner electric field

MPI

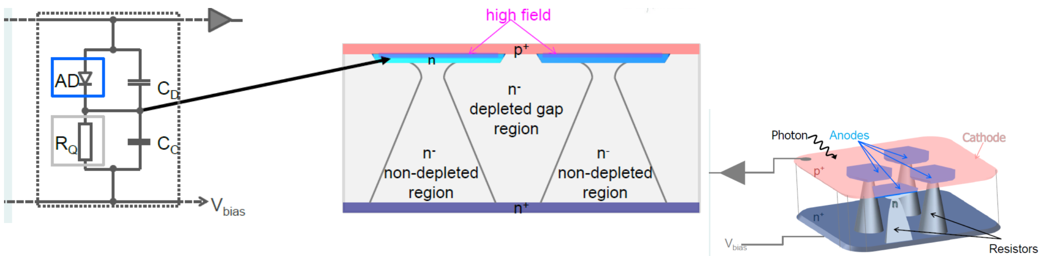

Ninkovic et al NIM A610 (2009) 142

NDL

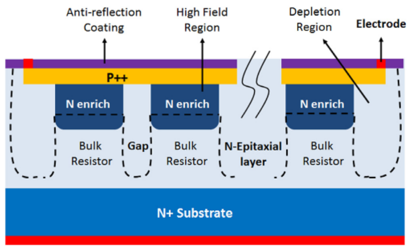

EQR-SiPM (3x3 mm², 9381 cells/mm²)

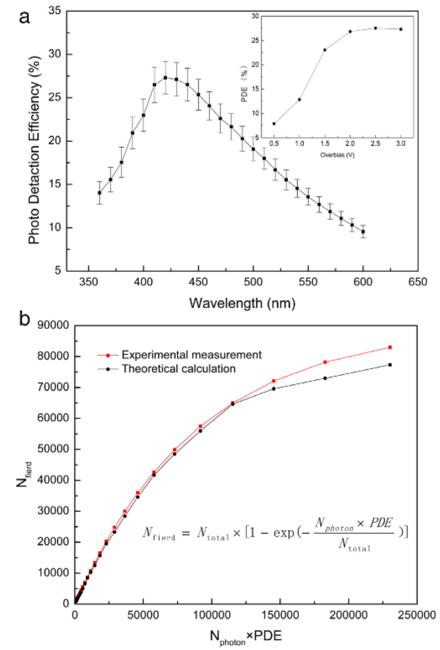

T. Zhao et al NIM A –In press

Advantages

- Production process simplified
- Entrance window free of any conduction lines → fill factor increasing
- The light entrance window is flat and can be easily covered with anti-reflecting coating
- High density of cells can be achieved

Drawbacks

- Non linear behavior with the voltage
- Longer recovery time than standard SiPM

R&D is still on going to improve this kind of devices

Active quenching: Digital SiPM

Use of a transistor to actively discharge/recharge the diode

dSiPM principle (Philips) : Instead of connecting each cell to a resistor, each cell of a dSiPM is connected to integrated electronics that actively quenches a breakdown and produces a binary signal.
The digital signal is then transferred to an :

✓ on-chip counter, which provides the number of detected photons

✓ a TDC, for the registration of the arrival time of the triggering photons

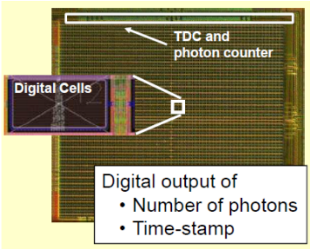

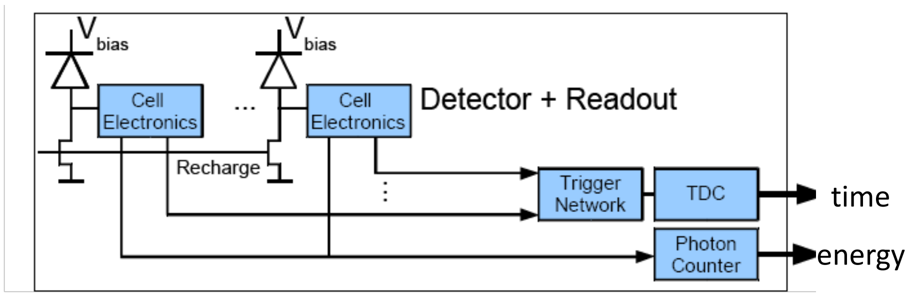

York Hämisch, TIPP 2011

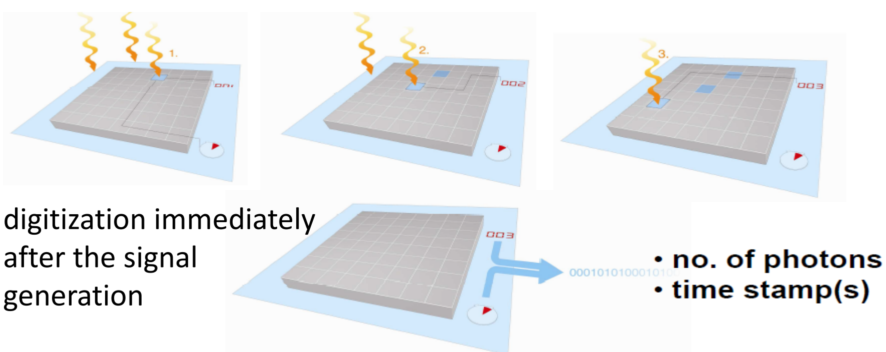

digital sum of the detected photons

Vertically integrated 3D SiPM

Array of GM-APD on a thinned silicon wafer (50 µm)

Each GM-APD is controlled and readout individually by a CMOS readout electronics which is placed under the detector (through a TSV)

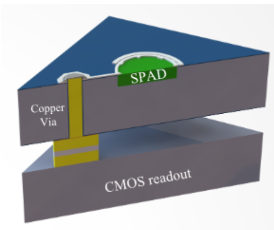

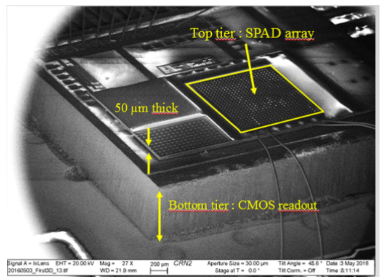

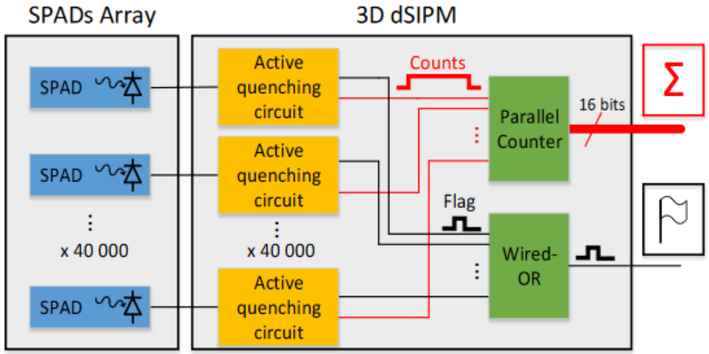

U.Sherbrooke :
- Photo detector tier design
- Electronics tier design
- 3D assembly

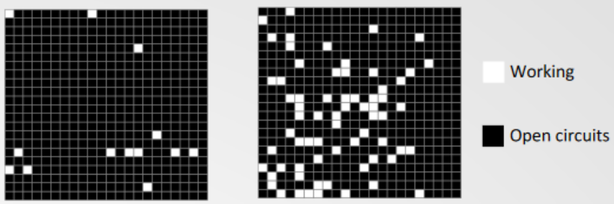

Proto1 : 13/484 pixels   Proto2 : 67/484 pixels

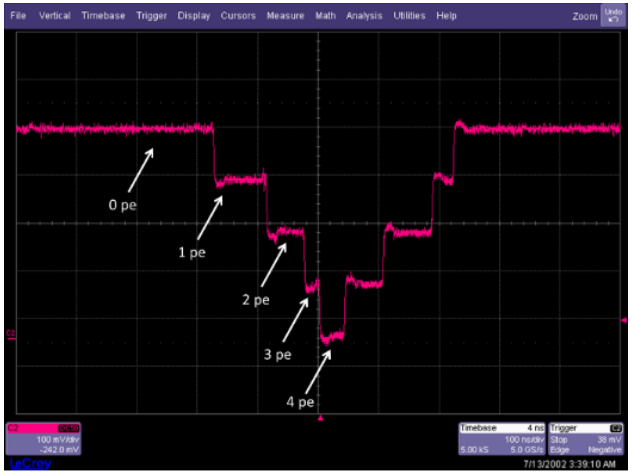

Light emission from SPAD turned OFF

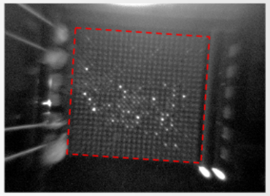

High-R paths – SPAD to TSV

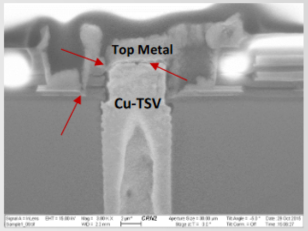

F. Retriere, TIPP 2017

Goal : Single Photoelectron Timing Resolution = 10 ps

Gain

Defined as the charge developed in one cell by a primary carrier

$$Gain = \frac{Q_{cell}}{e} = \frac{C_D \times (V_{bias} - V_{BD})}{e}$$

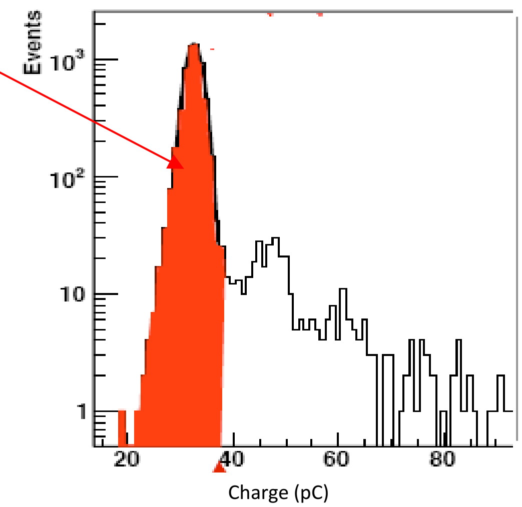

V_{BD}: bias at which occurs the breakdown

$\Delta V = V_{bias} - V_{BD}$

Gain of 1 mm² SiPM (25°C)

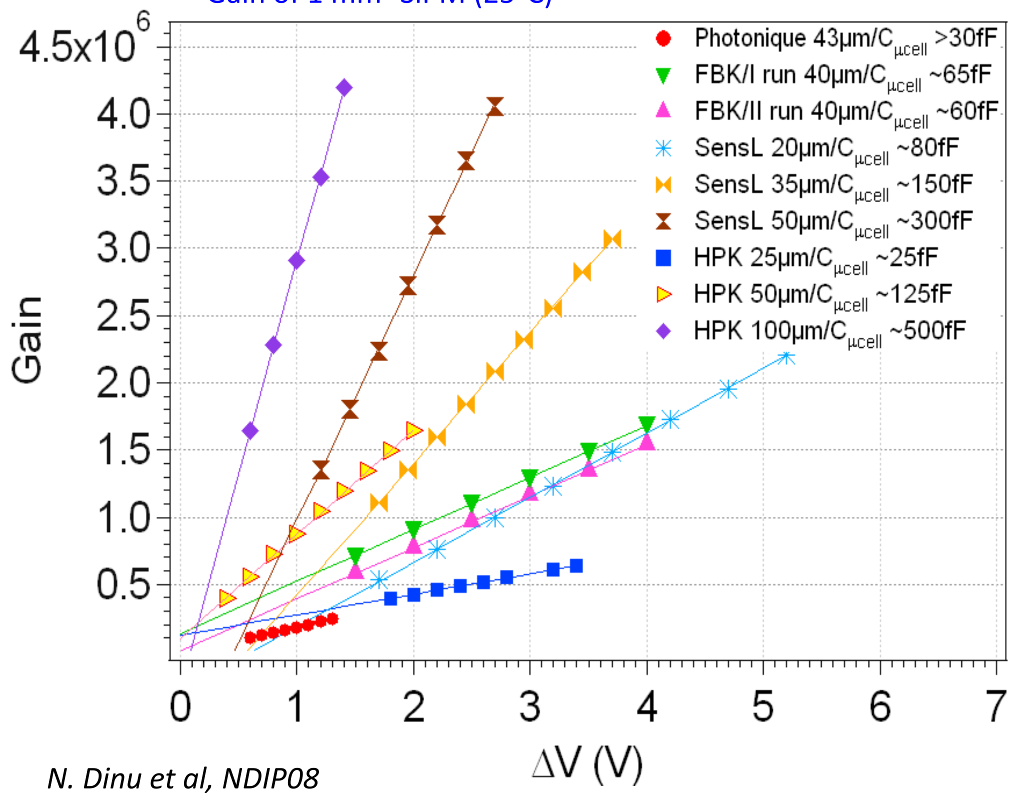

N. Dinu et al, NDIP08

10^5 < Gain < 10^6

- linear increase of the gain with Vbias
- slope of the linear fit of G as a function of Vbias → cell capacitance (tens to hundreds of fF)
- increase of the gain with the cell dimensions

Variation of the gain with the temperature

Temperature coefficients as a function of V_{bias}

Y. Musienko PoS(PD07)012

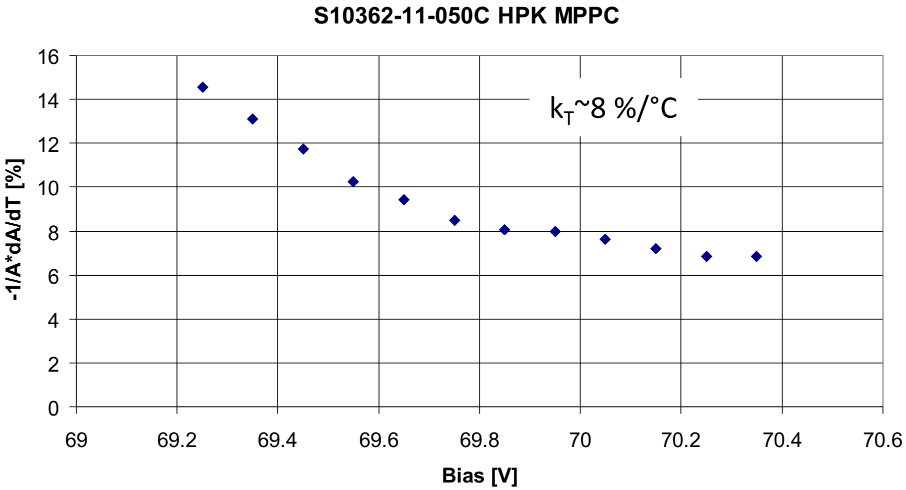

Gain independent of the temperature at fixed ΔV

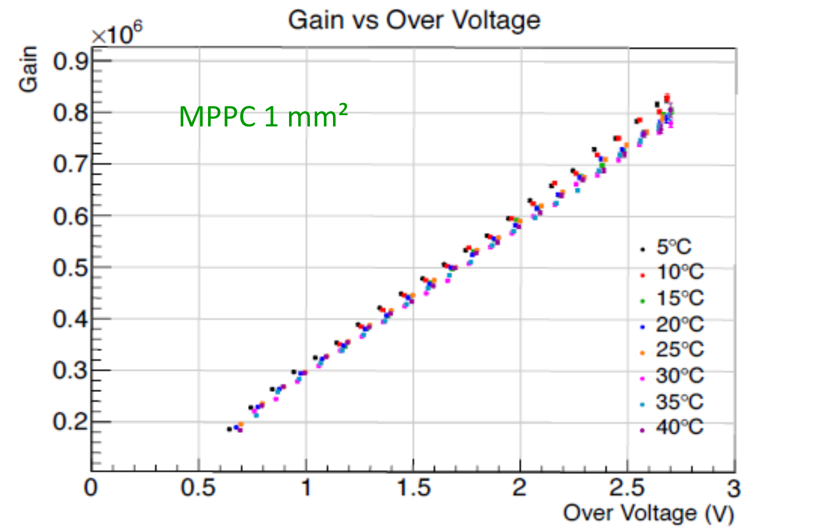

H. Tajima, 2013 CTA SiPM meeting

A. Tadday (UniHei)

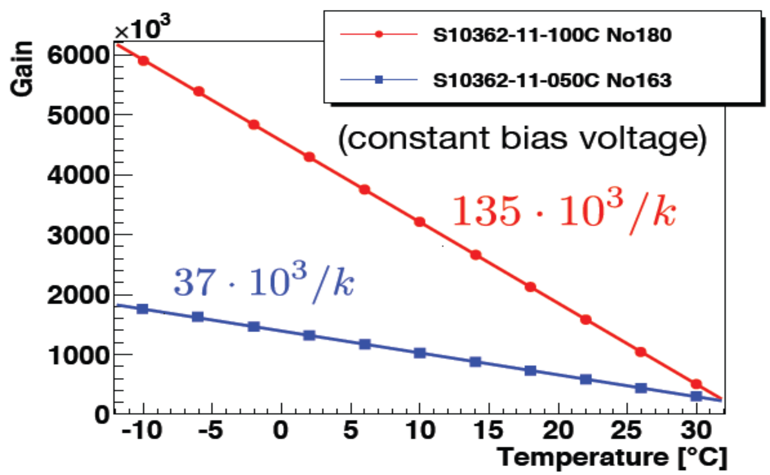

For a stable operation:

✓ the temperature needs to be controlled with a precision of a degree

✓ the over voltage as to be kept constant

The dependence of the gain with the temperature is larger with a bigger cell

Single photon detection performance

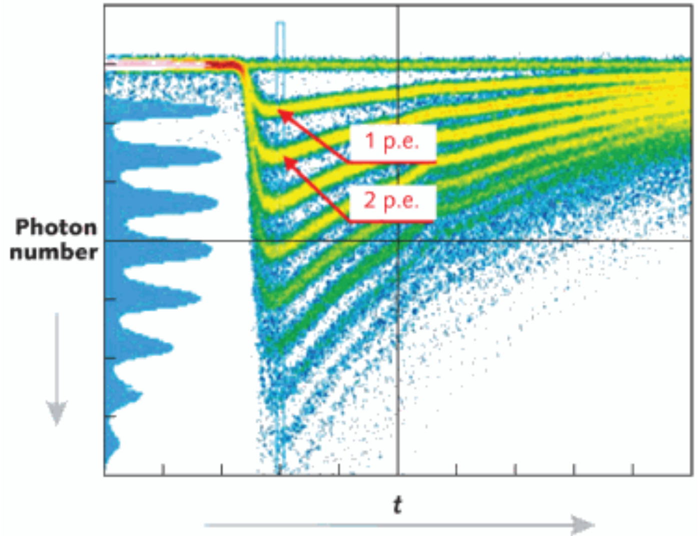

Signal distribution of the detecting the low photon flux by SiPM at room temperature

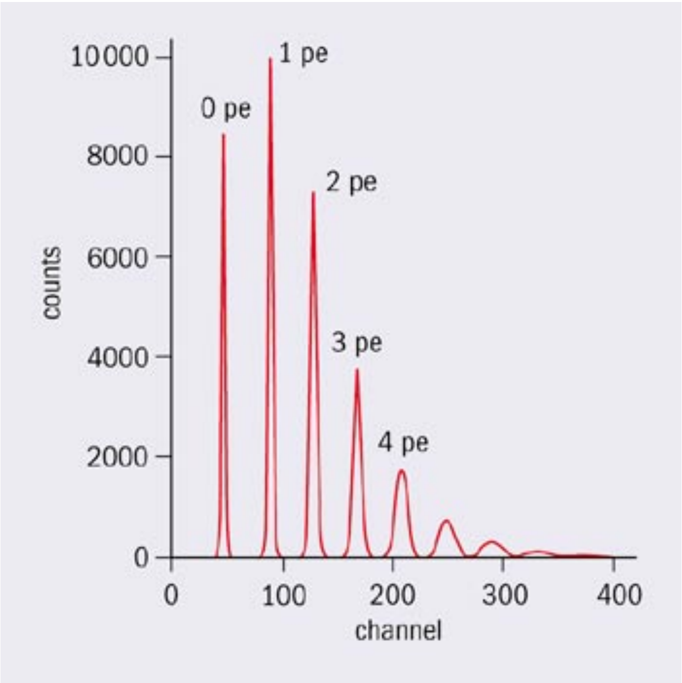

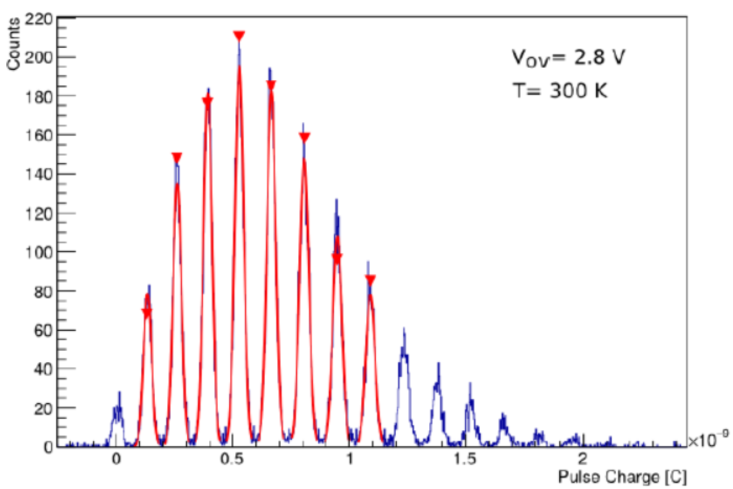

Single photons are well separated in a wide range

The resolution of SiPM allows very precise analysis of the detecting photon flux up to single photon

Photo Detection Efficiency (PDE - Qε)

$$PDE = Q_\varepsilon \cdot P_{trig} \cdot \ \varepsilon_{geom}$$

Qε: carrier Photo-generation

probability for a photon to generate a carrier that reaches the high field region in a cell

$$Q\varepsilon = (1 - R)\ \xi\ [1 - e^{-\alpha d}\ ]$$

fraction of the photon flux absorbed in the depleted layer (sensitive region). Depends on the thickness of this layer and of α

- ✓ effect of reflection at the surface of the device.
- ✓ reflection can be reduced by the use of antireflection coatings

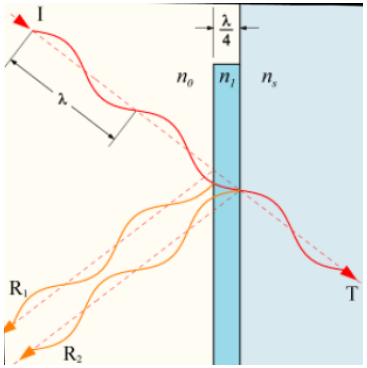

fraction of e-/h pairs that successfully avoid recombination at the Si surface and contribute to the useful photocurrent

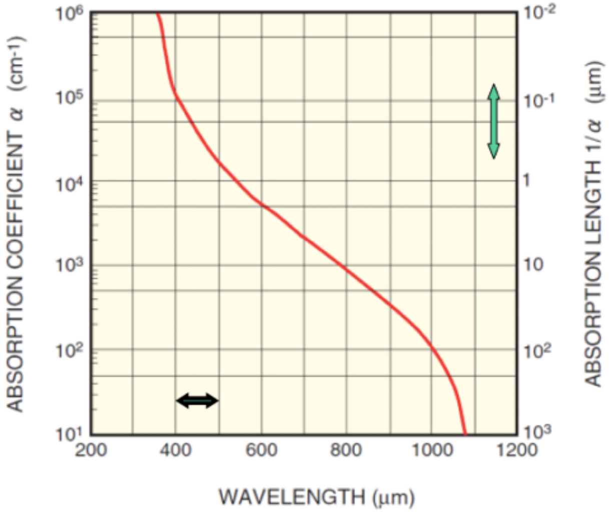

R : reflection Frenell coefficient = 0,3 for Si

Photo Detection Efficiency (PDE - P_{trig})

$$PDE = Q_{\varepsilon} \cdot P_{trig} \cdot \varepsilon_{geom}$$

Ptrig : avalanche triggering: probability for a carrier traversing the high-field to generate the avalanche
Depends on the position when the primary e/h pair is generated and of ΔV

e- directly collected at the n+ electrode → only the holes contribute to the avalanche

Hole directly collected at the p+ electrode → only the e- contribute to the avalanche

W.Oldham , IEEE TED (1972)

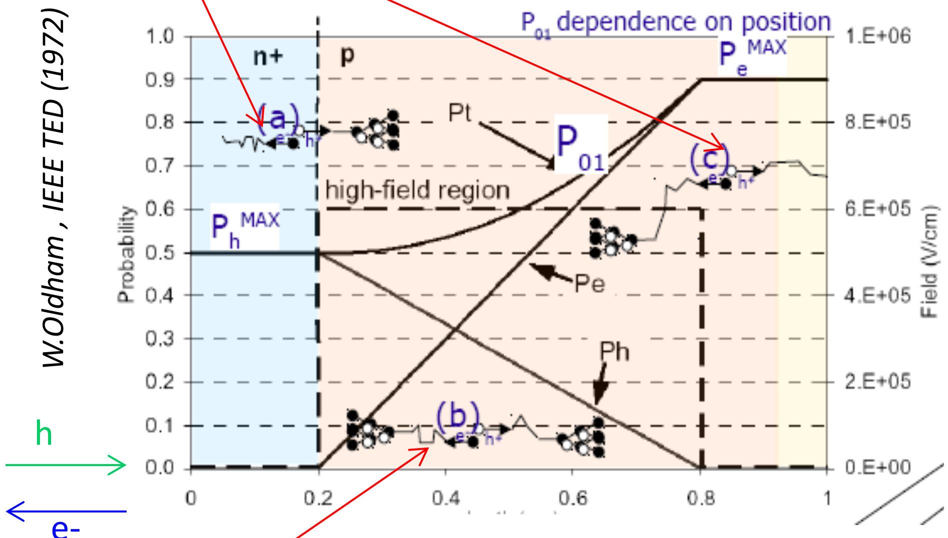

both carriers contribute to the avalanche

Ionization coefficients α for electrons and β for holes

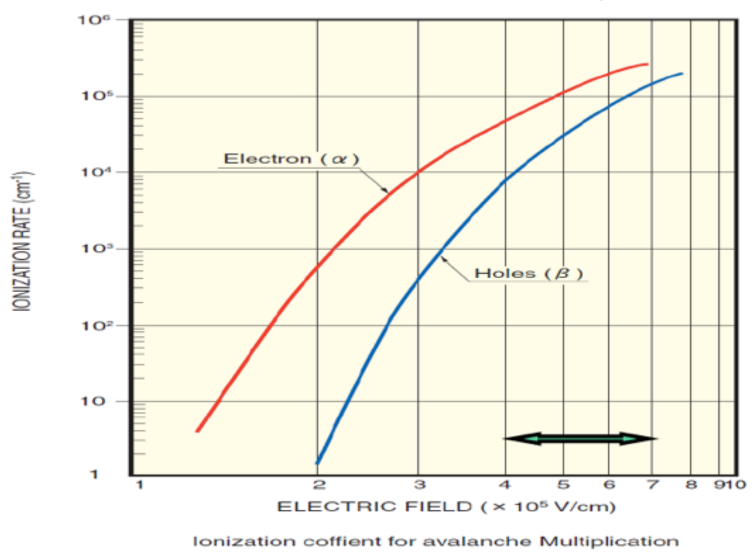

To maximize the triggering probability, the photon conversion should happen in the p side of the junction, in order to allow the electrons to cross the high-field zone and trigger the avalanche

Photo Detection Efficiency (PDE - ε_{geom})

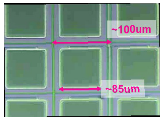

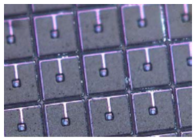

$$PDE = Q_{\varepsilon} \cdot P_{trig} \cdot \varepsilon_{geom}$$

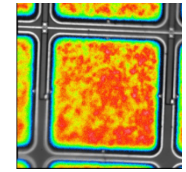

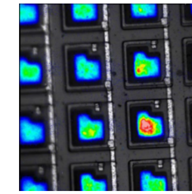

ε_{geom} : geometrical Fill Factor

fraction of the sensitive to insensitive area. Only part of the area occupied by the cell is active and the rest is used for the quenching resistor and other connections

How to increase the Fill factor ?

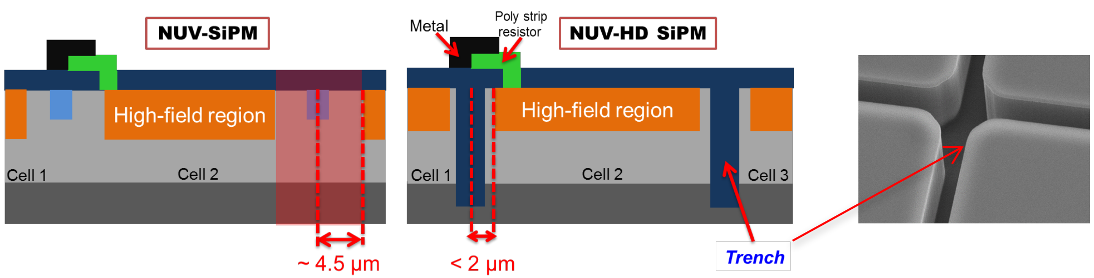

FBK High-Density technology:
Etching thinner trenches between the cells →smaller dead border region → higher Fill Factor (30 % increase)

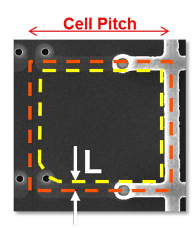

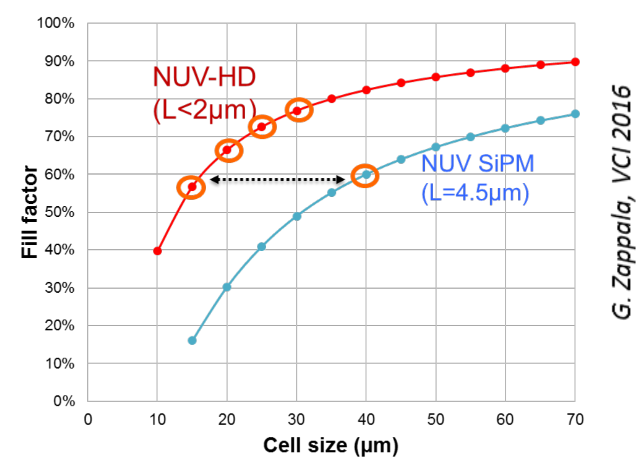

PDE of SiPMs: p-on-n structure

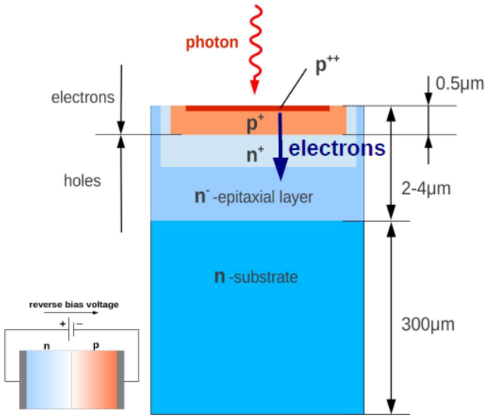

Blue photons absorbed in the first µm→ only the e- drift toward the high field of the junction and trigger an avalanche with high probability.

In the case of longer λ, holes will drift toward the junction with smaller triggering proba → reduced PDE

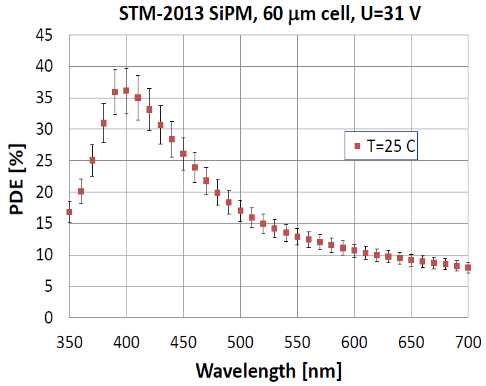

Y. Musienko, INSTR14

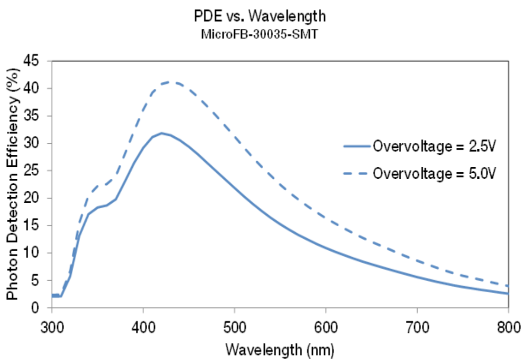

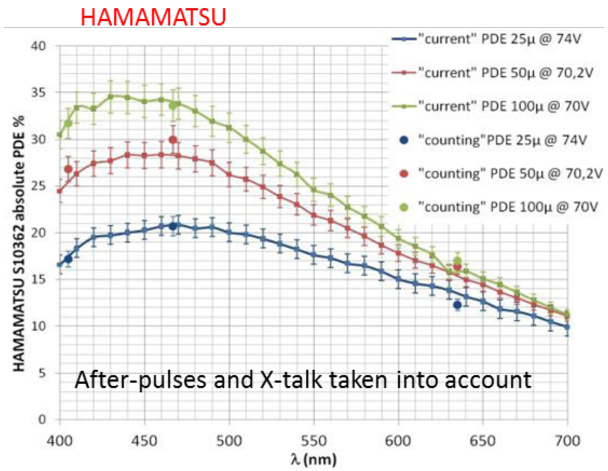

V. Chaumat, PoS (PhotoDet 2012) 058

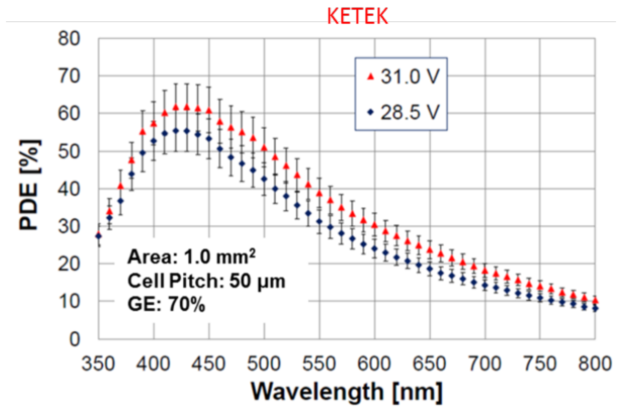

F.Wiest – AIDA 2012

p-on-n SiPM with shallow junction exhibits higer PDE value in the blue region (e- trigger avalanches at short λ)

PDE of SiPMs: n-on-p structure

n-on-p SiPM with larger depletion depth have higher sensitivity in the red

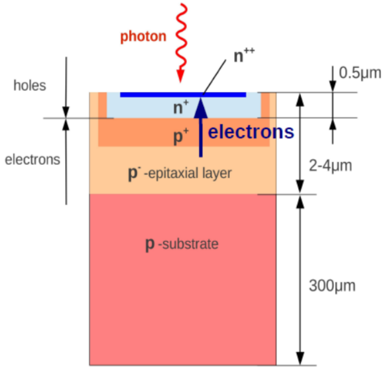

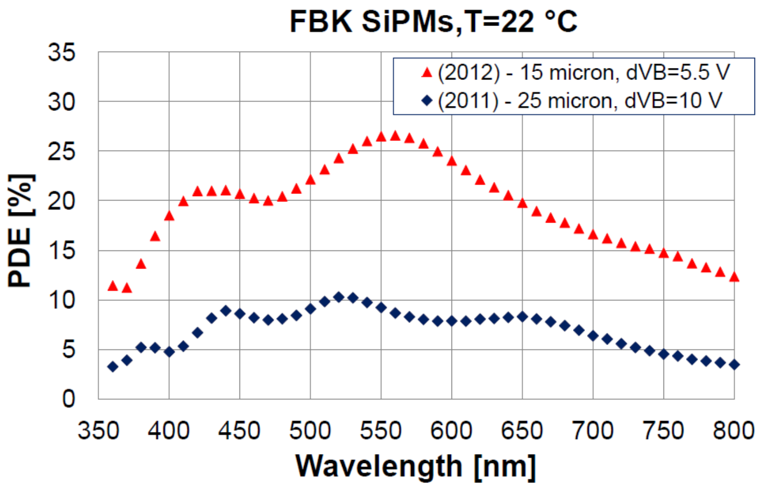

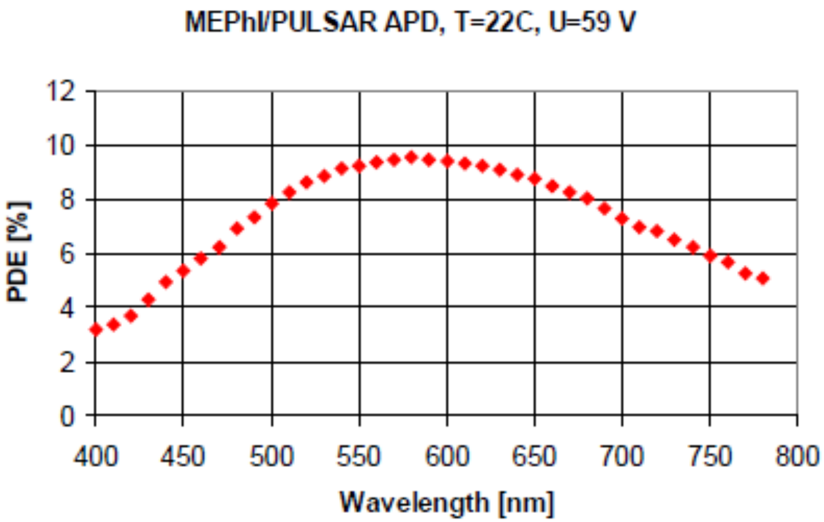

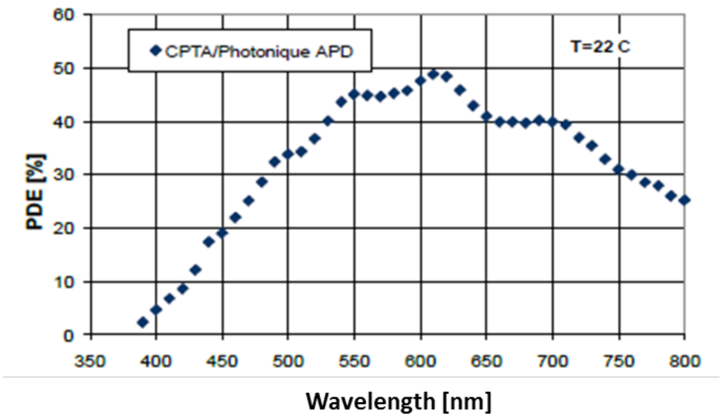

Y. Musienko, INSTR14

VUV SiPMs

PDE for VUV is ≈ 0 for commercial devices because of :

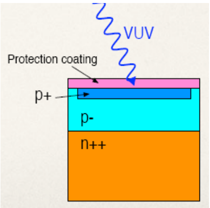

- low transmission for these λ of the sensitive layer which is due to the protection coating (epoxy resin/silicon rubber) that absorbs the photons
- as the absorption length in Si is 5 nm for UV photons, they are absorbed in the p+ layer just below the surface
- high index of reflection for UV photons on Si surface

HAMAMATSU

SiPMs sensitive to VUV light (<150 nm) were recently developed by HPK for detection of LAr (T=-186 °C) scintillation light (λ = 128 nm).

- precise control of MPPC's protection layer
- optimization of the MPPC parameters (less defects)

→ reduction the recombination of carrier produced just under the surface

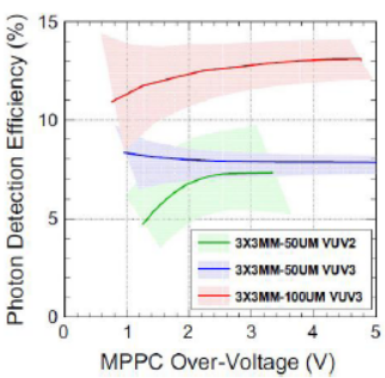

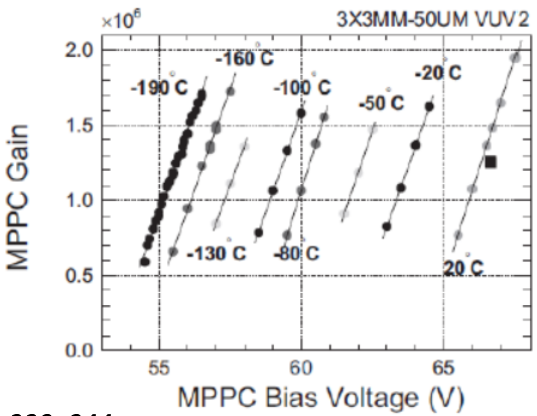

NIM A833 (2016) 239–244

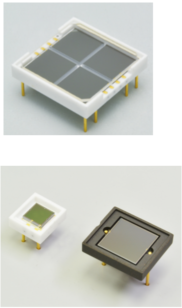

New VUV MPPC

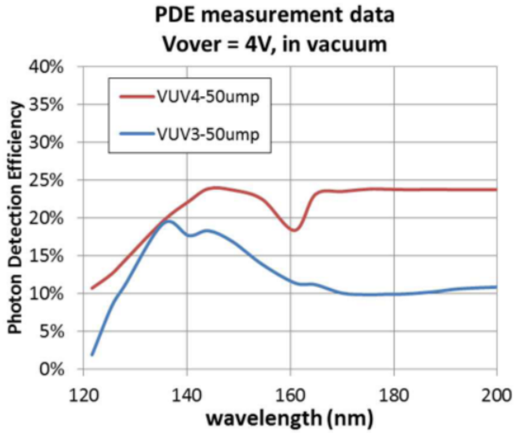

HAMAMATSU, private communication

NUV SiPMs

FBK

SiPMs sensitive to NUV light (λ = 178 nm).

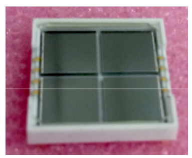

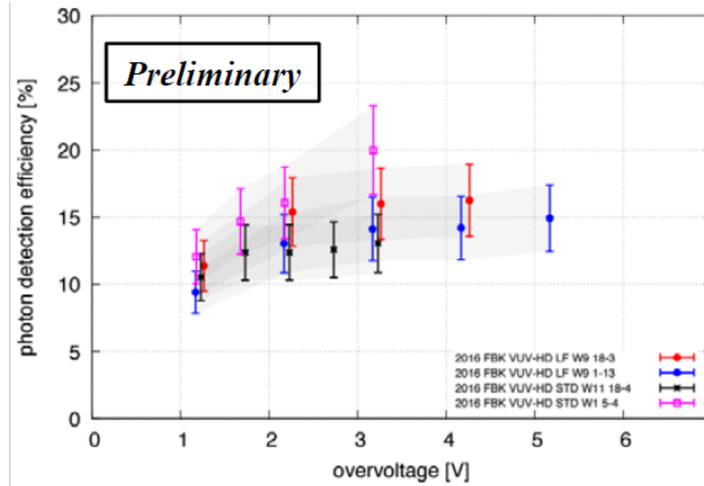

X. Sun, NDIP17

Noise sources of a SiPM

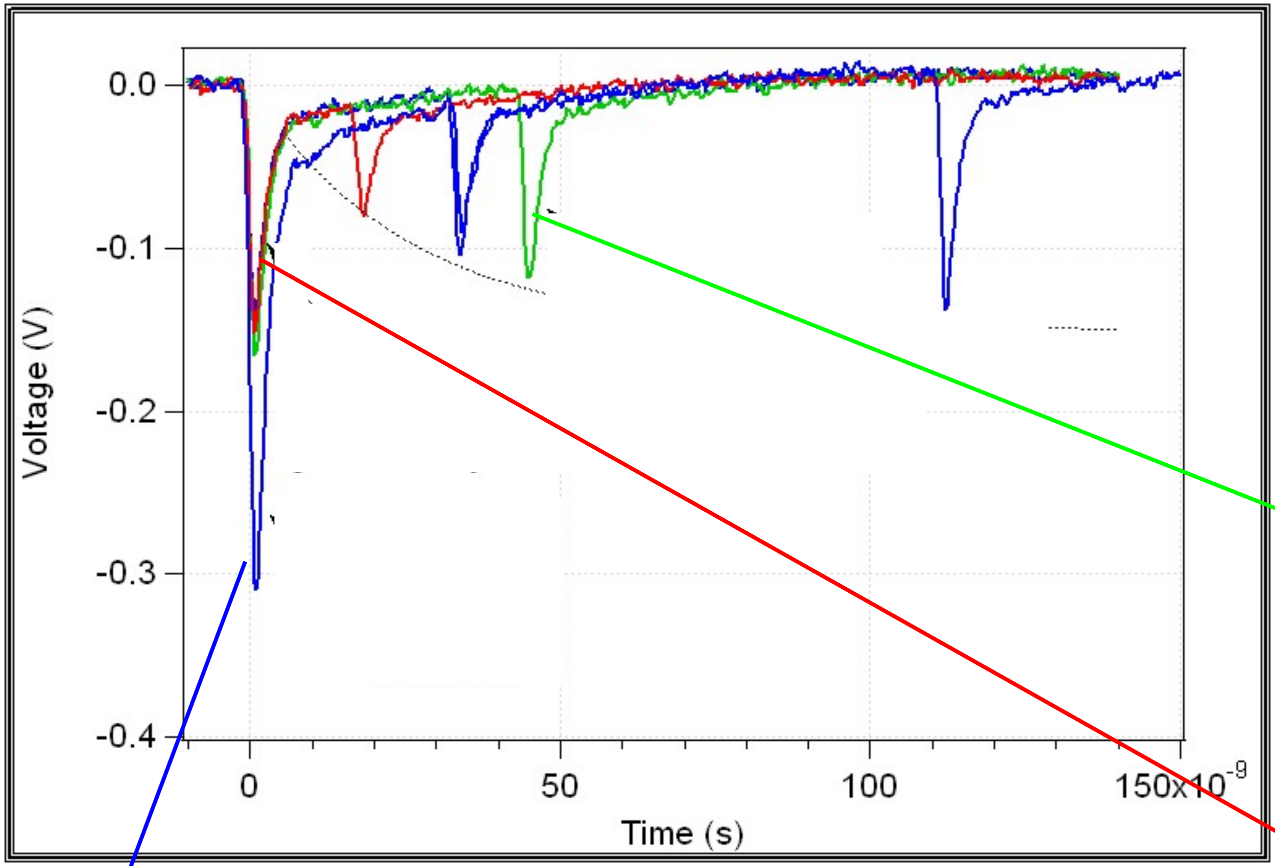

Contribution 2: After-pulses

carriers trapped during the avalanche can produce delayed secondary pulses

Contribution 1: Dark counts

pulses triggered by non-photo-generated carriers (thermal / tunneling generation in the bulk or in the surface depleted region around the junction)

Contribution 3: Cross-talk : amplitude = 2 p.e

avalanche in one cell → proba that a photon triggers another avalanche in a neighboring cell without delay

Dark Count rate (DCR)

Average frequency of the thermally generated avalanches breakdown process that result in a current pulse indistinguishable from a pulse produced by the detection of a photon.

BEFORE

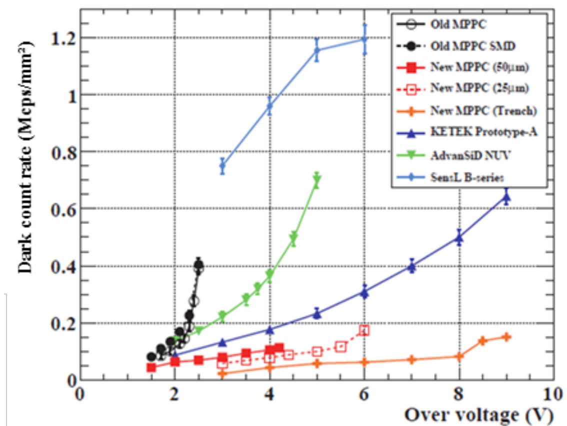

Y.Uchiyama et al, IEEE NSS 2013

DCR dSiPM & analog SiPM

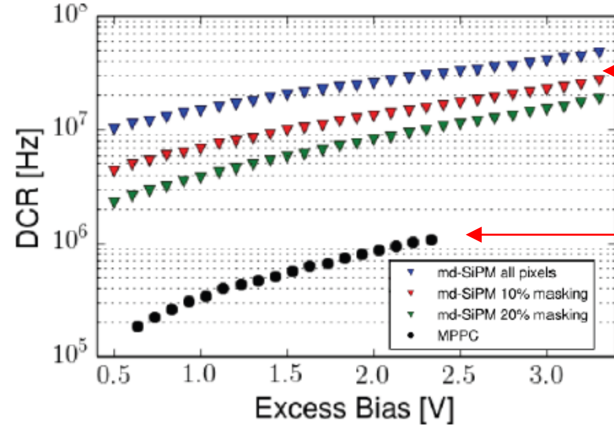

TODAY

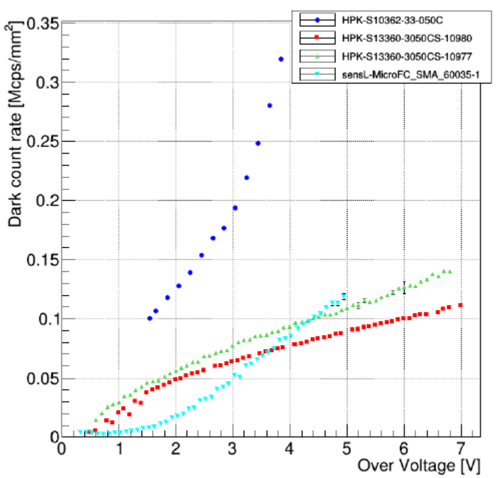

C. Betancourt, Siena worksop 2016

Pixel by pixel DCR of dSiPM (TU Delft)

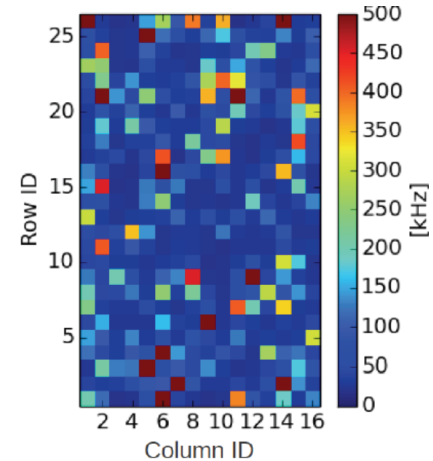

DCR of recent devices ≈ few 10 kHz/mm²

Variation of the DCR

Variation with the bias voltage and the temperature

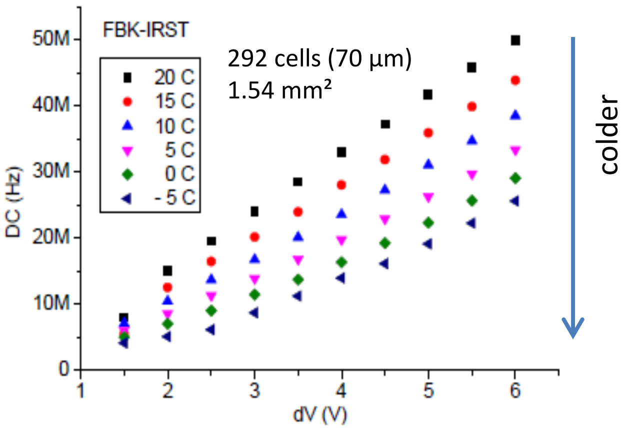

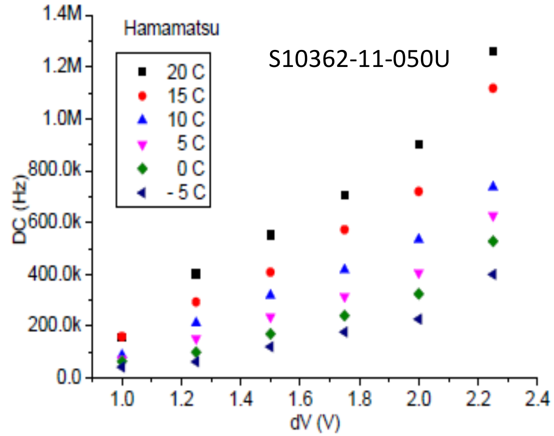

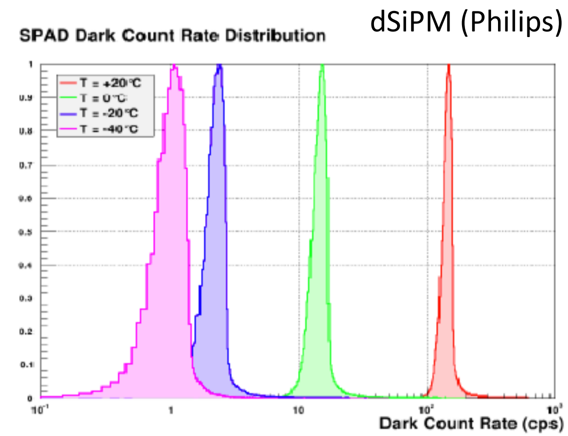

O. Starodubtsev, PoS 2012

Increase of the DCR with the increase of the bias voltage and the temperature

Best way to decrease the Dark Count rate:

✓ operate the SiPM at low bias voltage

✓ cooling (factor ≈ 2 reduction of the dark counts every 8°C)

After-pulses

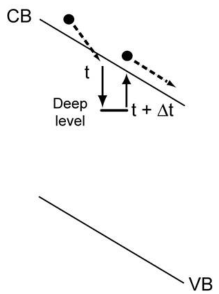

Formation in the Si volume where a breakdown happened of a plasma with high temperatures (a few 1000 °C) → deep-lying traps in the Si creation → carriers can be trapped

They may be released at some time and trigger a new breakdown avalanche event : afterpulse (described in term of probability)

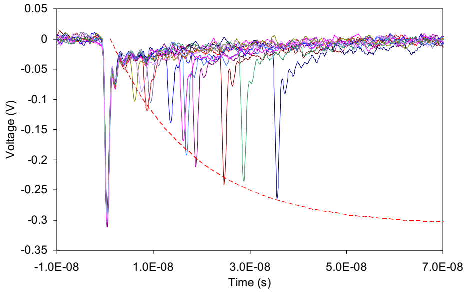

$$P_{afterpulse}(t) = P_{trig} \times P_{capture} \frac{e^{-t/\tau}}{\tau}$$

$P_{capture}$: trap capture proba

P_{trig}: avalanche triggering proba

τ: trap lifetime

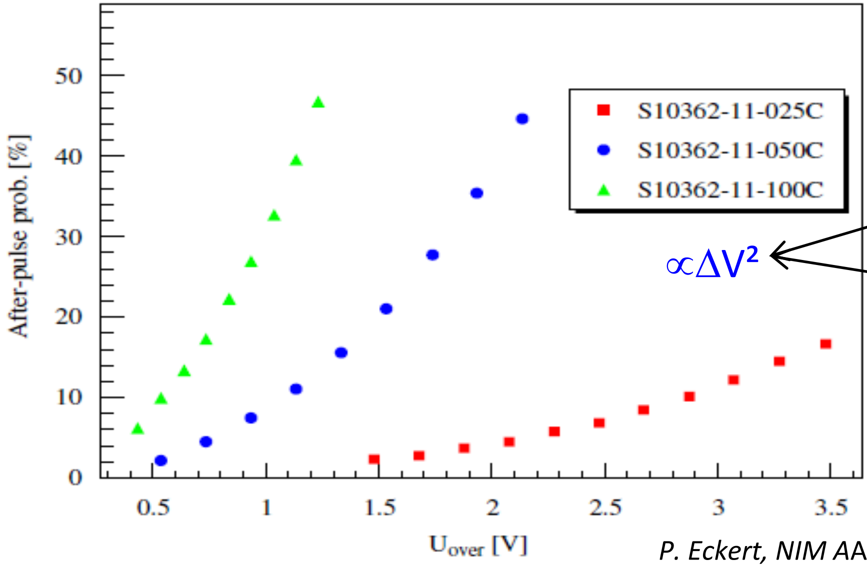

Number of carriers produced in the avalanche ∝ ΔV

Triggering proba ∝ ΔV

P. Eckert, NIM AA 620 (2010)

How to decrease the afterpulsing ?

Impurities (Iron, Gold) and defects (point, dislocation) create deep levels in the band gap

Minimization of the amount of impurities in the avalanche region employing pure Si wafers and new process conditions.

HAMAMATSU before after

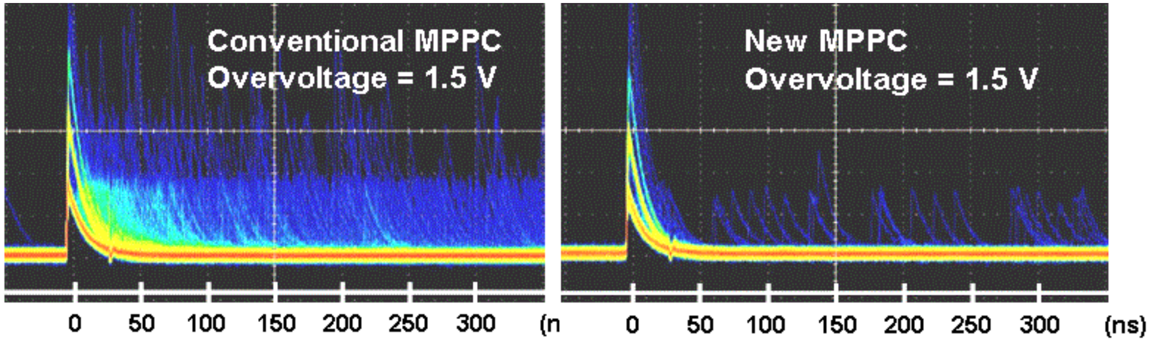

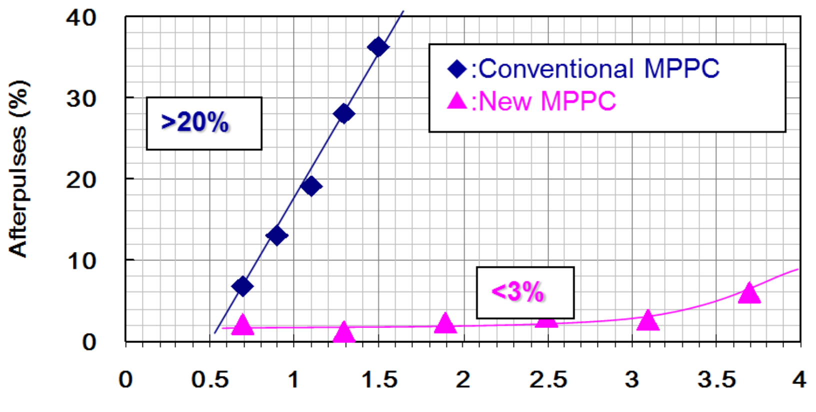

K. Sato, VCI 2013

FBK

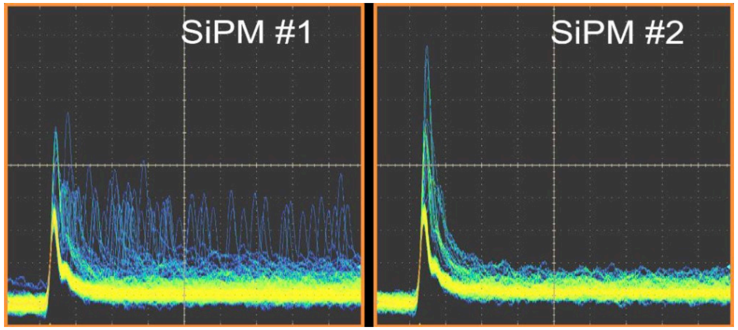

F. Acerbi, PhotoDet2015

Cross-talk

avalanche in one cell probability than 1 carrier emits IR photons with E > 1.12 eV

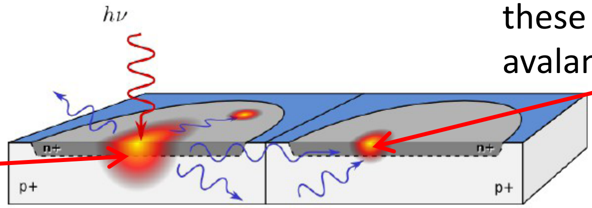

these photons (≈ 30 for a gain of 10^6) can trigger another avalanche in a neighboring cell without delay

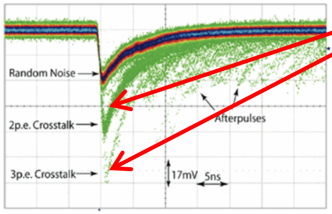

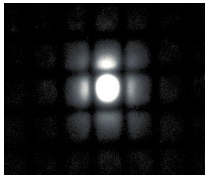

M. Knötig, 2nd SiPM workshop 2014

Ways in which secondary photons can travel to neighboring cells to cause optical Xtalk

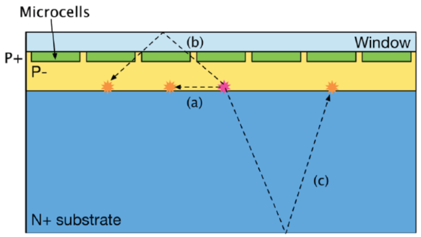

a) directory to a neighboring cell

b) reflected from the window material on the top of the sensor (usually epoxy or glass)

c) reflected from the bottom of the silicon

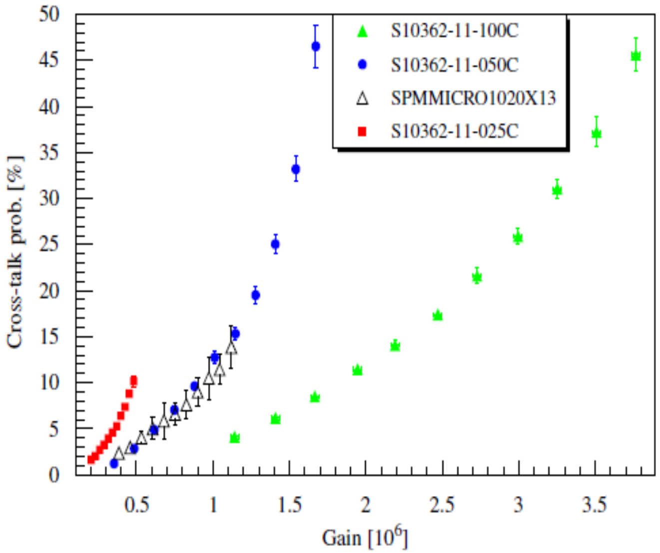

P. Eckert, NIM AA 620 (2010)

- Xtalk probability increases with the dimension of the cell
- rises with the bias voltage (number of produced charge carriers)

How to decrease the Cross-talk

One solution to decrease the X-talk : optical isolation between the cells by etching trenches filled with opaque material

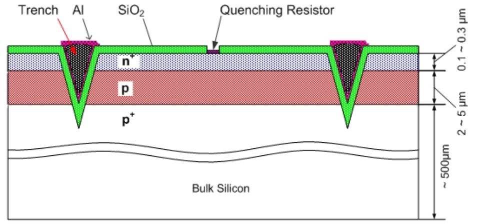

D. McNally, G-APD workshop (2009)

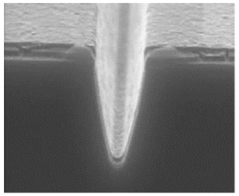

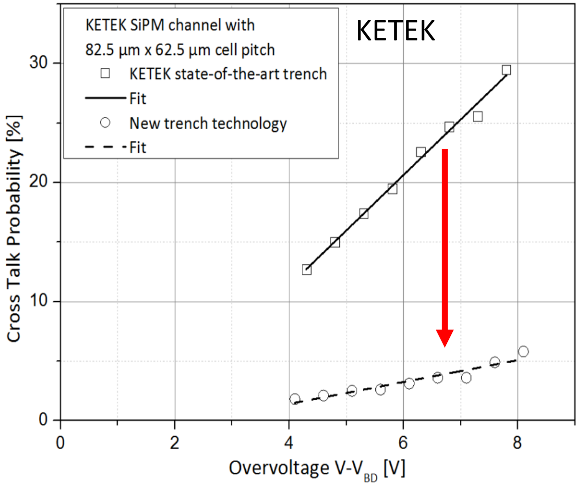

KETEK – Photodet-2015

HAMAMATSU HD-1015CN

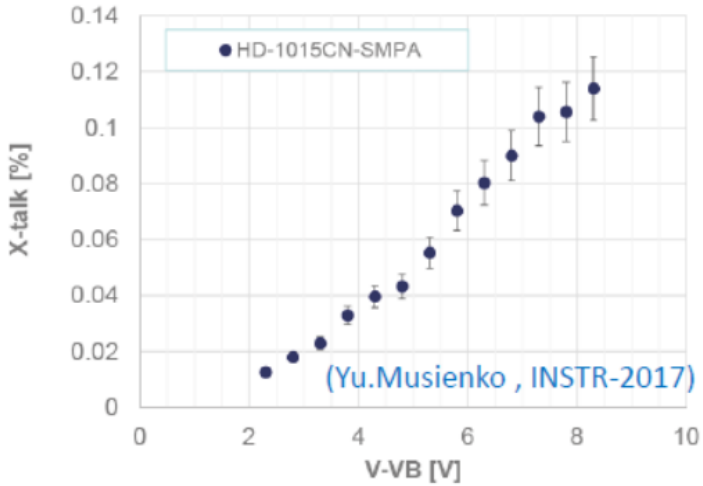

Xtalk < 0.1 % !!!

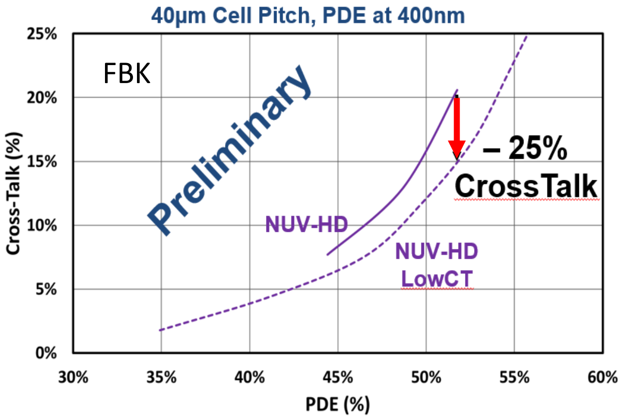

G. Zappalà, VCI-2016

Time response of SiPMs

Active layer is very thin (few µm) → breakdown development is very fast + big charge → we can expect very good timing properties even for single photons

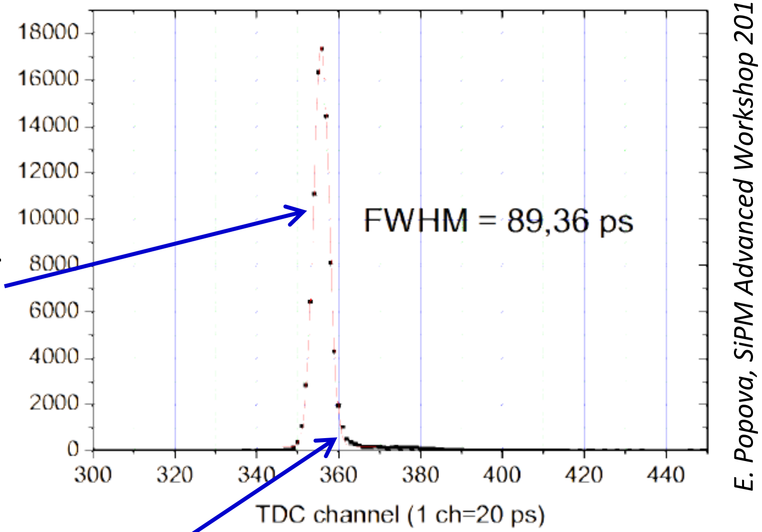

fast component of Gaussian shape with 50 ps< σ < 150 ps
The fluctuation are due to the variance of the transverse diffusion speed and the variance of transverse position of photo-generation.

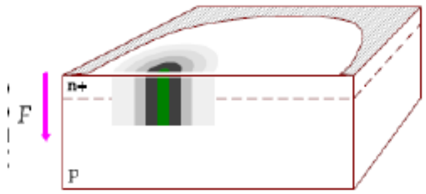

Transverse multiplication

slow component: minor non Gaussian tail
with time scale of several ns due to minority carriers, photo-generated in the neutral regions beneath the depletion layer that reach the junction by diffusion (~$L^2/\pi D$ with L effective neutral layer thickness and D, diffusion coefficient)

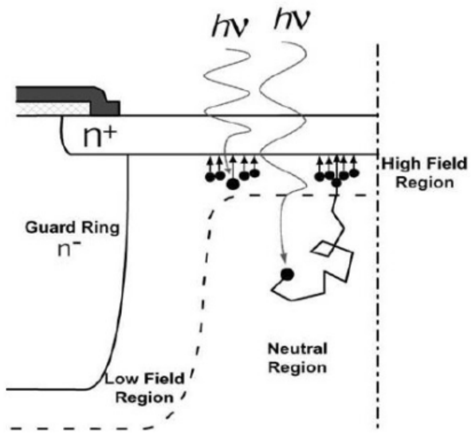

Variation of the timing resolution

The precision of a SiPM in determining the time of arrival of a single photon is referred to as the SPTR: Single Photoelectron Timing Resolution (FWHM or σ)

Variation with the interaction position in the cell

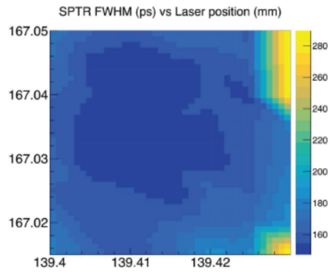

FBK NUV SiPM 3x3mm²

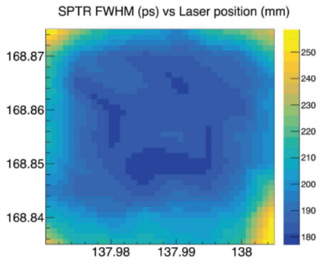

Hamamatsu TSV SiPM 2x2mm²

M.V. Nemallapudi, JINST 11 P10016

1 mm²

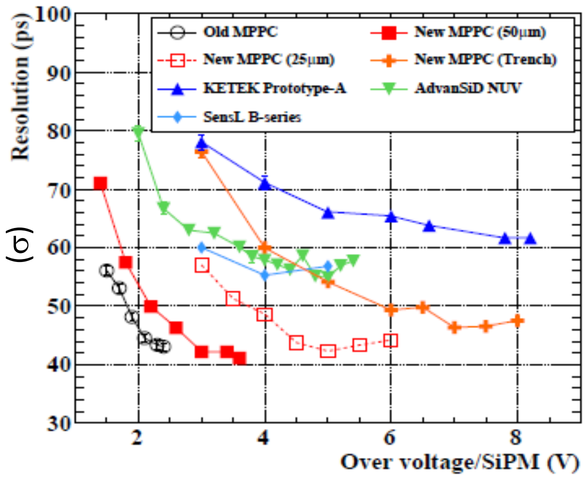

P.W Cattaneo, arXiv:1402.1404v1

4 to 16 mm²

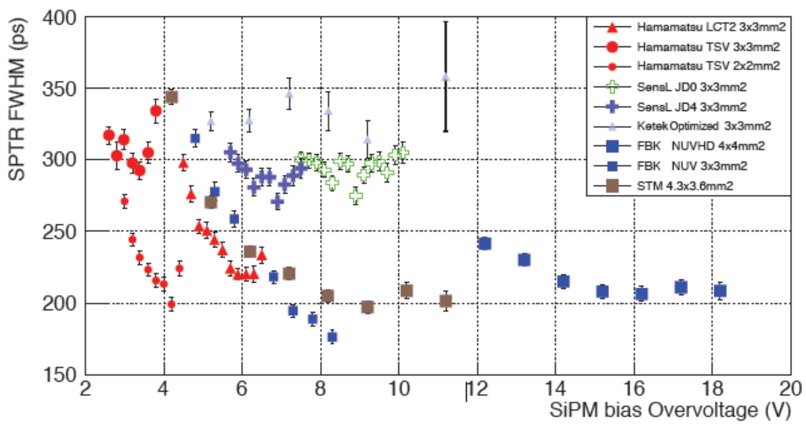

M.V. Nemallapudi, JINST 11 P10016

Variation of the timing resolution

SPTR as a function of the temperature (-220 to 25°C)

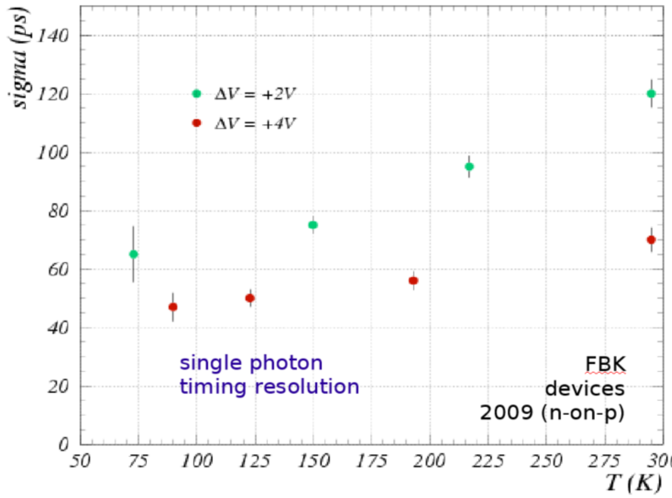

G. Collazuol, IEEE NSS 2016

At low temperature, higher carriers mobility

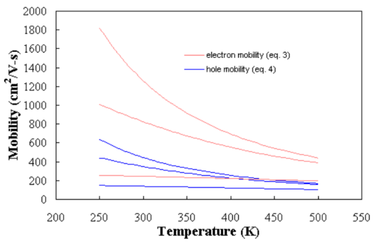

→ avalanche process is faster and fluctuations are reduced

Timing resolution as a function of the incident number of photons

Poisson statistics: $\sigma_t \propto 1/\sqrt{N_{pe}}$

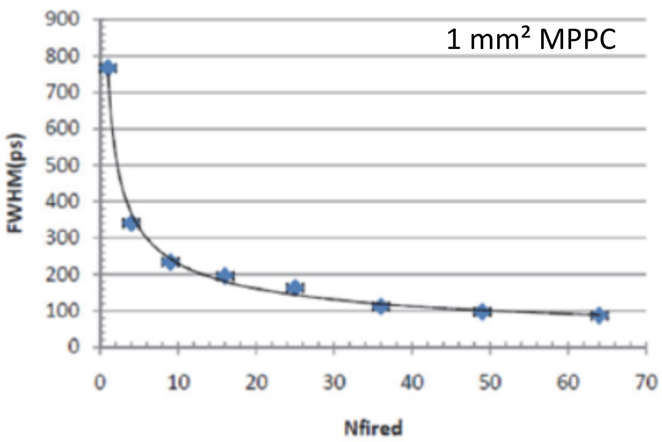

G. Barbarino, DOI: 10.5772/21521

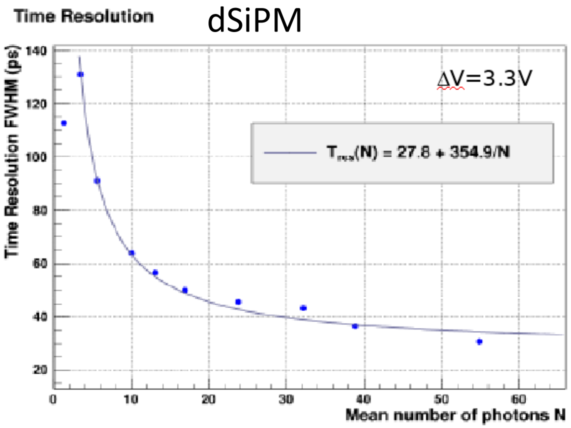

T.Frach, LIGHT 2011

Dynamic range and linearity

Detection of photons: statistical process based on the probability of detecting randomly distributed photons by a limited number of cells→ the dynamic range is determined by the PDE and the total number of cells

$$N_{firedcells} = N_{total} \cdot (1 - e^{-\frac{N_{photon} \cdot PDE}{N_{total}}})$$

$N_{firedcells}$: number of excited cells
N_{total}: total number of cells
N_{photon}: number of incident photons in a pulse

2 or more photons in 1 cell look exactly like 1 single photon

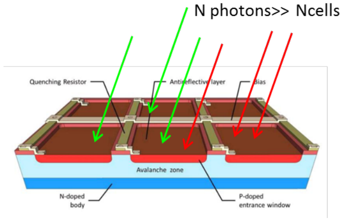

Output signal: proportional to the number of fired cells as long as

N_{photon} x PDE << N_{total}

SiPM response as a function of the number of instantaneous incident photons

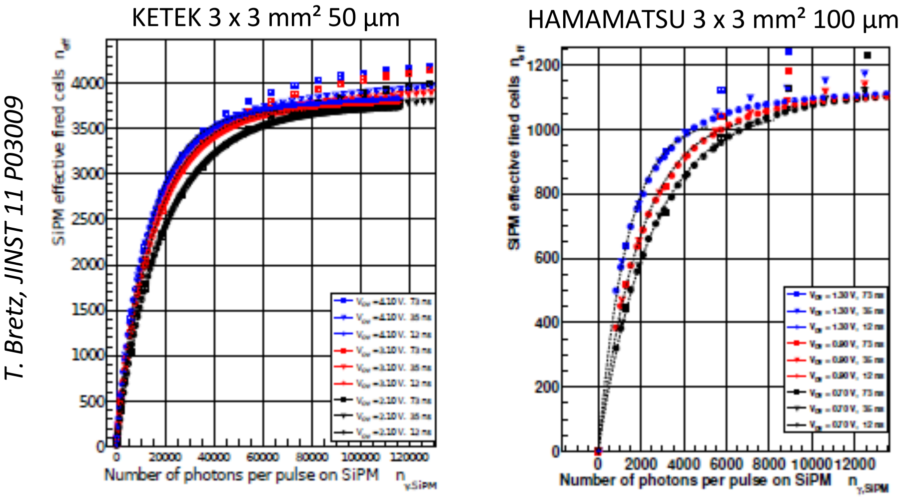

The saturation is a limiting factor for the use of SiPM where large dynamic range of signal (5000 – 10000 photons/pulse) has to be detected (calorimetry)

Solution to the saturation: large number of cells

high density SiPM : device with more than 1000 cells/mm² + short recovery time

HAMAMATSU

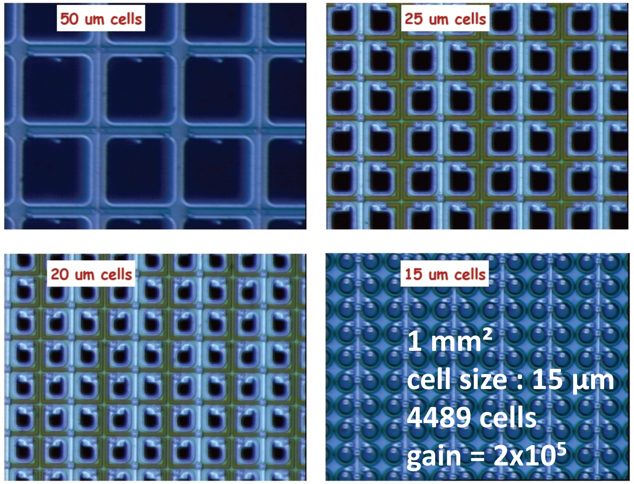

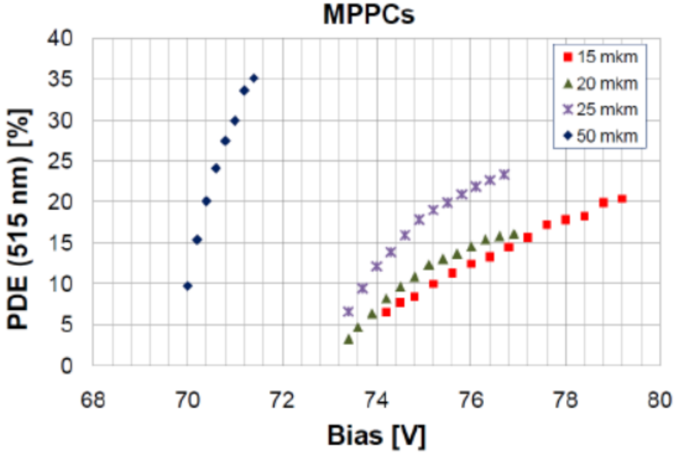

Y.Musienko, CTA SiPM Workshop, 2014

50 µm   10 µm

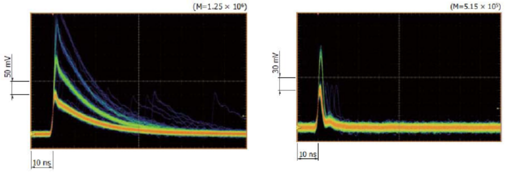

GREEN: MPPC B1-15um   BLUE: MPPC B1-20um
ORANGE: MPPC B2-15um   RED: MPPC B2-20um

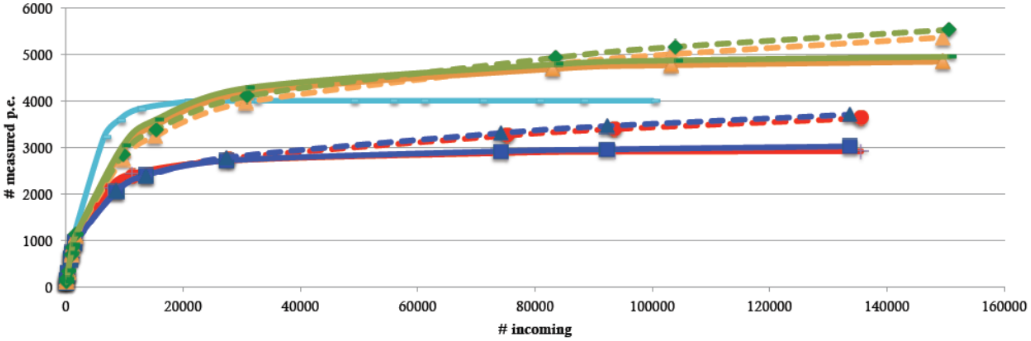

E. van der Kraaij , LCD ECAL meeting 2014

Drawback : PDE lower than the one of standard device due to the deterioration of the fill factor.

Solution to the saturation: large number of cells

FBK

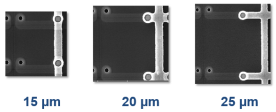

Cell Pitch	FF	Cell Density
15 µm	55 %	~4444 cells/mm²
20 µm	66 %	2500 cells/mm²
25 µm	73 %	1600 cells/mm²
30 µm	77 %	~1111 cells/mm²

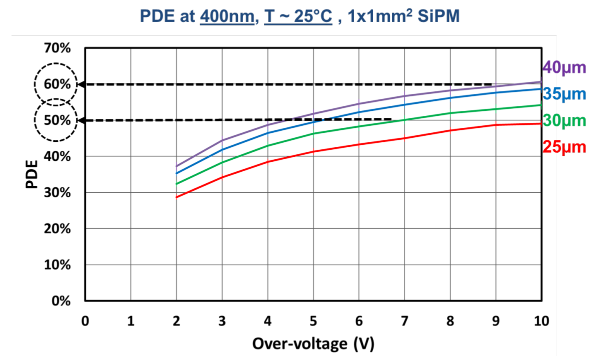

G. Zappalà, VCI-2016

NUV-HD

- PDE (350 nm) = 40 % @ ΔV=3 V
- DCR = 80 kHz@ 20°C (ΔV = 3V)

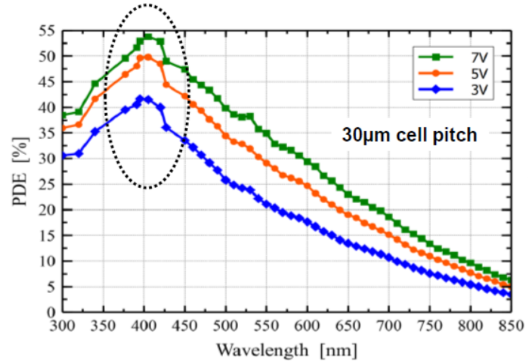

F. Acerbi, PhotoDet2015

KETEK

high density SiPM : device with more than 8000 cells/mm²

MP15 V6 W8:
1.2x1.2 mm²
Cell size = 15 µm
12800 cells

MP20 V4 W12:
3x3 mm²
Cell size = 20 µm
22500 cells

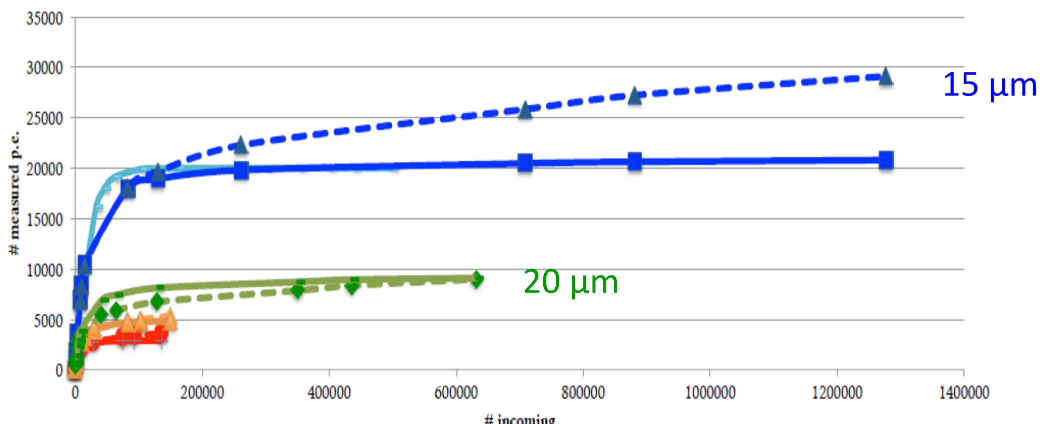

E. van der Kraaij, LCD ECAL meeting 2014

Solution to the saturation: very large number of cells

ZECOTEK MAPD-3N

The quenching resistors are formed in the epitaxial Si rather than on the surface of the device

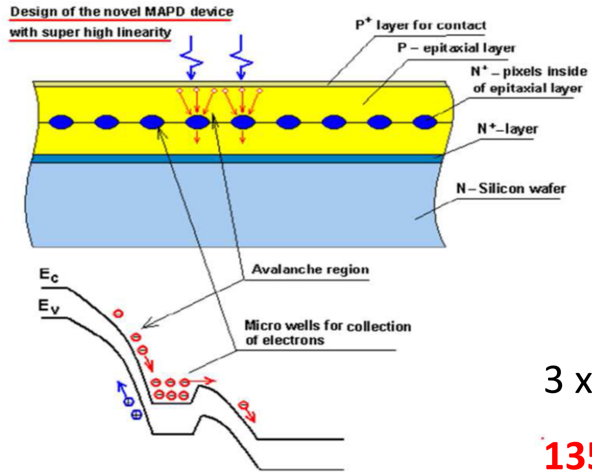

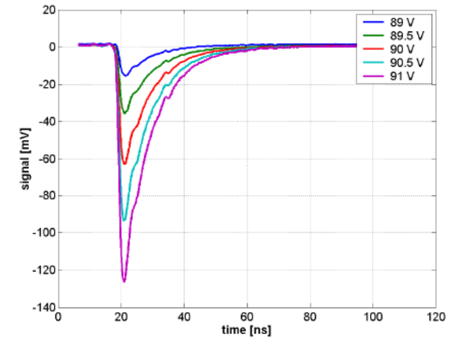

A. Rychter, Proc. of SPIE Vol. 8454

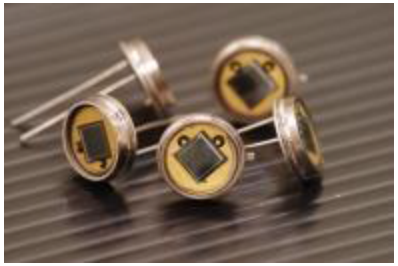

3 x 3 mm²

1350000 cells (15000/mm²)

gain = 10^5

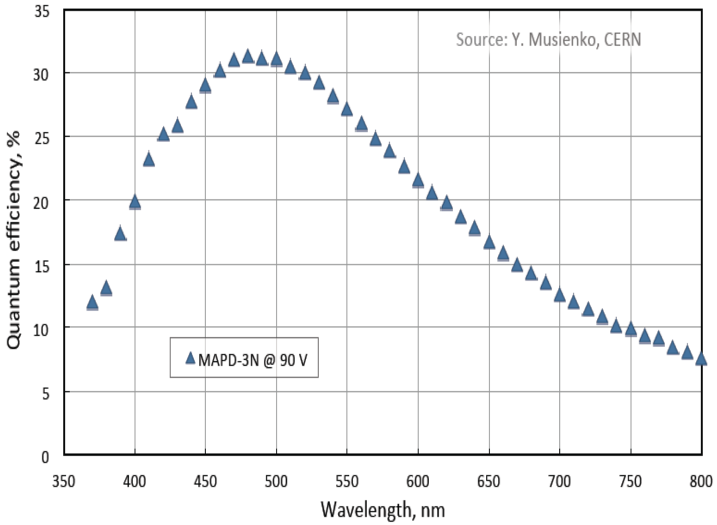

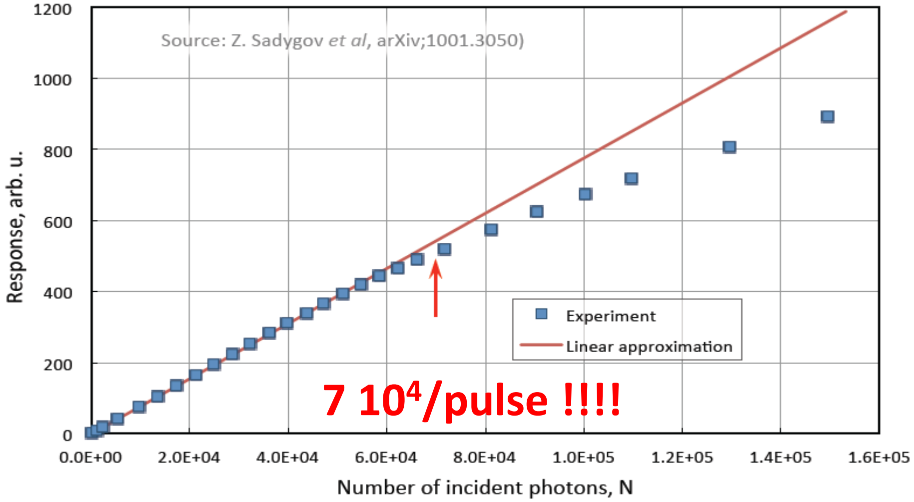

Radiation damages on SiPMs

protons / neutrons

bulk damages caused by lattice defects

γ-rays, X-rays

creation of trapped charges near the Si-insulator interface

Ionization damage can be caused by hadrons as well as X and γ and can produce different effects in the SiPMs

- increase of the dark current
- change of the breakdown voltage
- change of the gain and PDE dependence as a function of bias voltage

❖ limitation of the low light detection capability
❖ destruction of the device

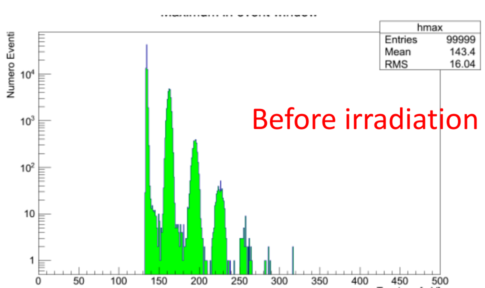

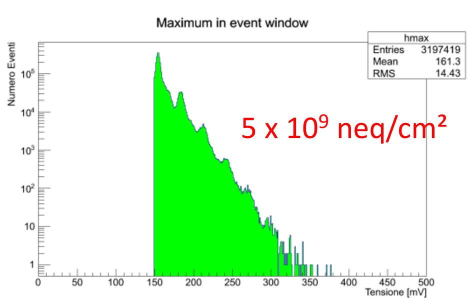

DCR

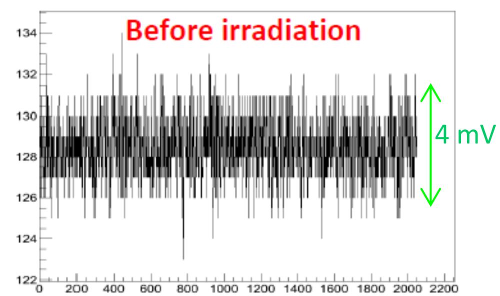

DCR

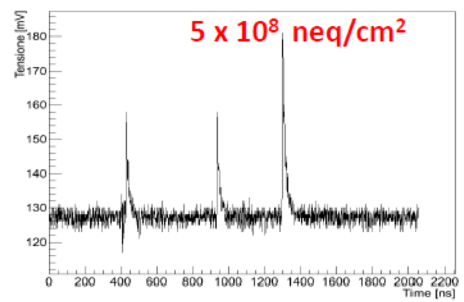

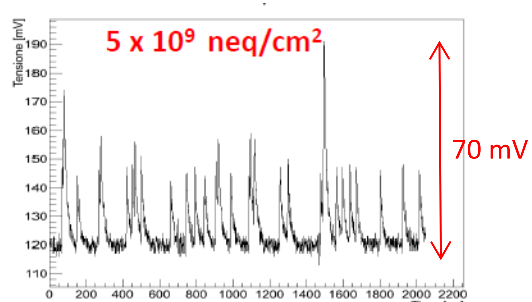

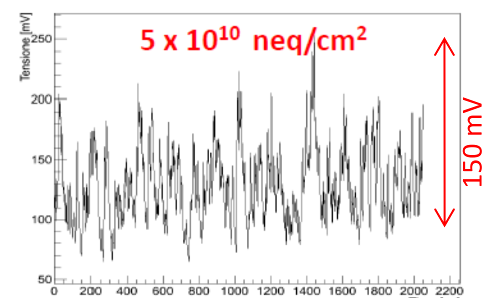

W. Baldini, TIPP 2014

Resistance to neutron irradiation

BEFORE

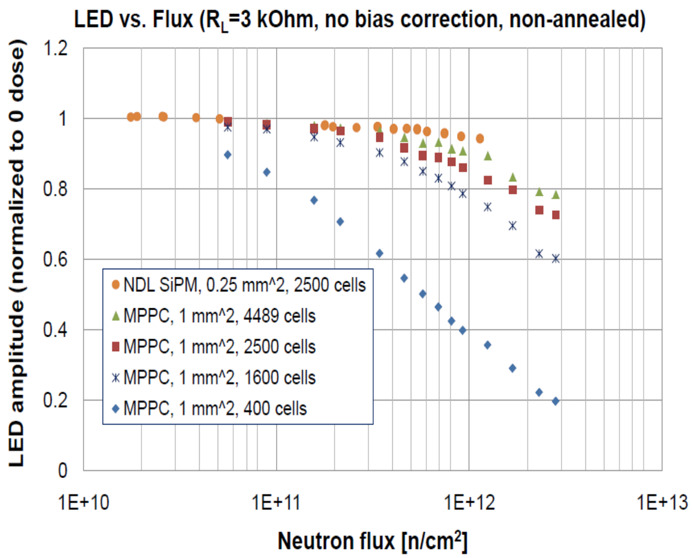

J. Anderson CALOR 2012

- no change of V_{BD} (within 50 mV accuracy)
- significant increase of the DCR
- SiPMs with high cell density and fast recovery time can operate up to 10^{12} n/cm² ($\Delta G < 25\%$)

TODAY

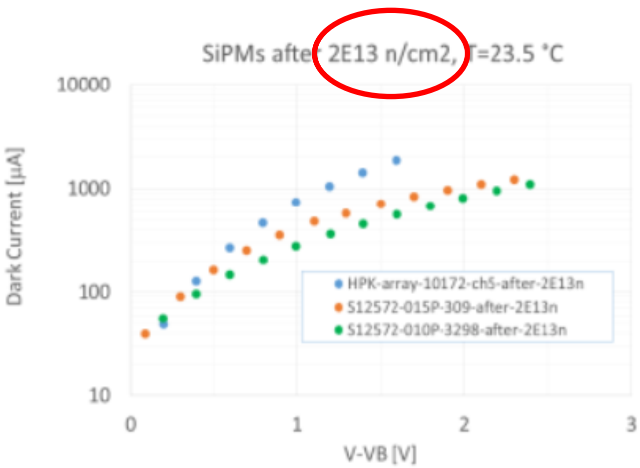

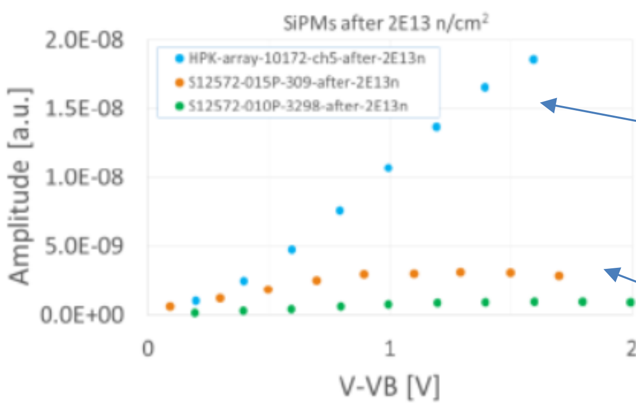

HAMAMATSU devices

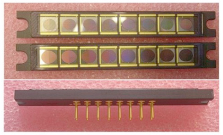

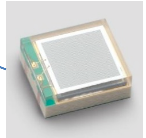

A.Heering, IEEE NSS 2016

Resistance to neutron irradiation

Can SiPM survive very high neutron fluences expected at high luminosity LHC?

FBK SiPM (1 mm², 12 µm cell pitch) was irradiated with 62 MeV protons up to **$2.2*10^{14}$n /cm²** (1 MeV equivalent)

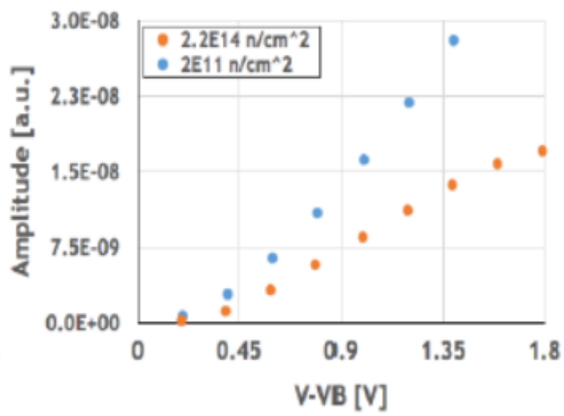

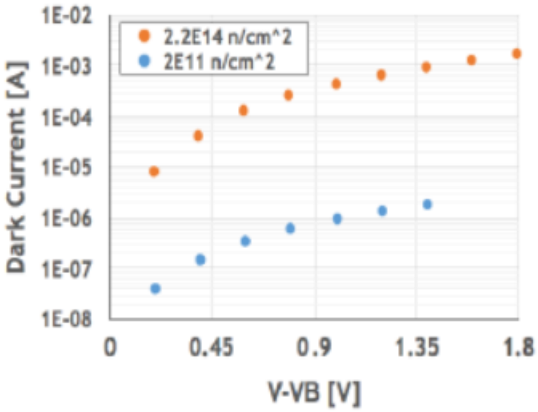

A.Heering, NIM A824 (2016) 111

- Increase of V_{BD}: ~0.5 V
- Drop of the amplitude (~2 times)
- Reduction of PDE (from 10% to 7.5 %)
- Increase of the current (up to ~ 1 mA at ΔV=1.5 V)

SiPM survived this dose of irradiation and can be used as photon detector!

Irradiation by protons 800 MeV/c of dSiPM

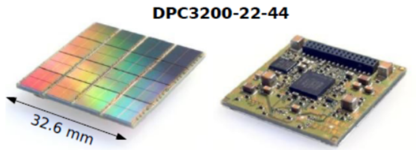

Array of 4x4 die.
Die = 128x100 cells (Geiger-mode APDs) + + TDC (LSB=20ps) + 4 photon counters.

Active cell quenching.
Full digital data output.
Noisy cells can be disabled.

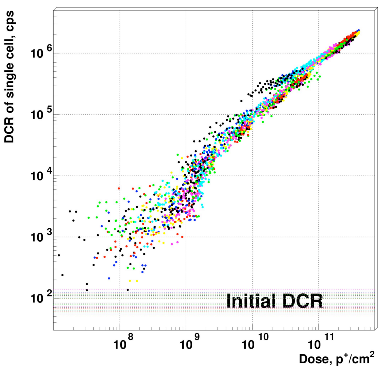

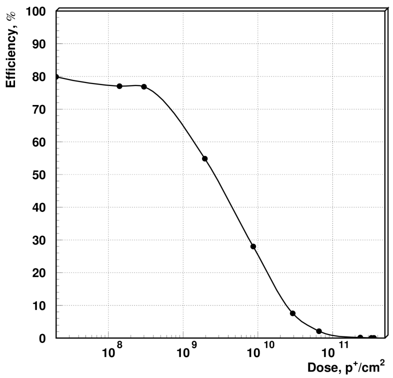

M.Barnyakov , Elba 2015

Recovery at low temperature

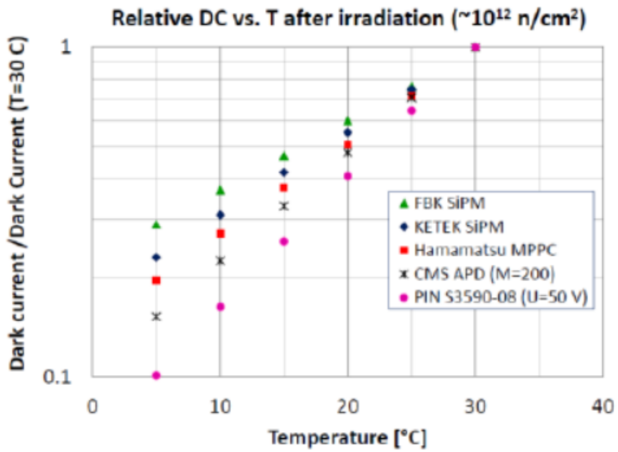

Y.Musienko, NDIP14

Normalized Id for new and irradiated SiPM

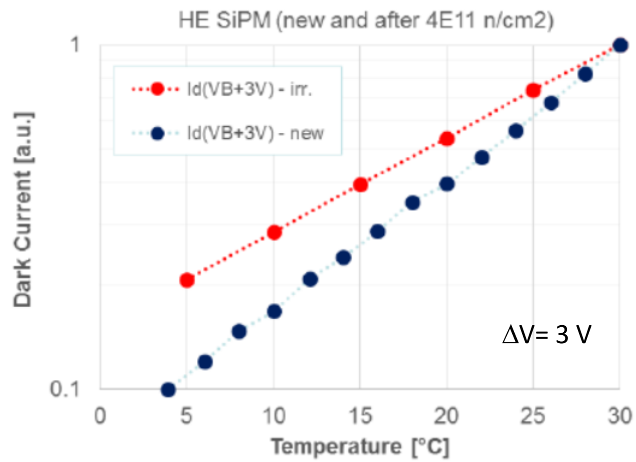

SiPM after 2.10^{13} n/cm² at reduced temperature

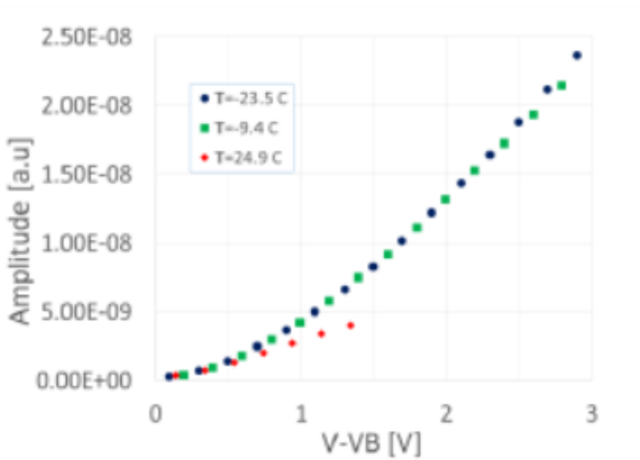

A.Heering, IEEE NSS 2016

- Irradiated HE MPPC, Id reduction: ~1.9 times/10 °C
- Non-irradiated HE MPPC, Id reduction: ~2.4 times/10 °C

- At -9.4 °C SiPM response recovers to that of non-irradiated SiPM
- From 24.9 °C to -23.5 °C: ~21 times Id reduction

How to extend the lifetime of SiPM after irradiation?

SiPMs cooled to 5°C during the irradiation→ reduction of the dark noise by a factor 3

Beam down period : SiPMs heated to ~40°C (post-irradiation annealing) → bring the noise down to a residual level (in 24 h instead of 5 days at room temperature)

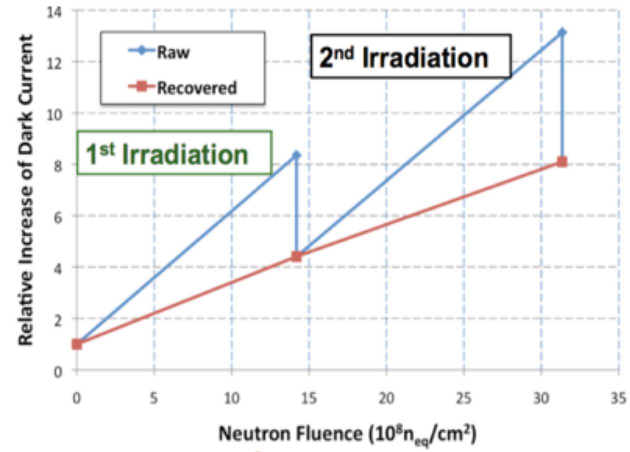

F. Barbosa, BNL 2011 conference

Hot annealing at 160°C after an irradiation at 10^{12} n/cm² → DCR & single-photon detection performance recovered

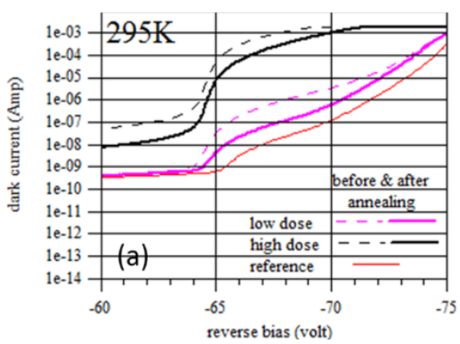

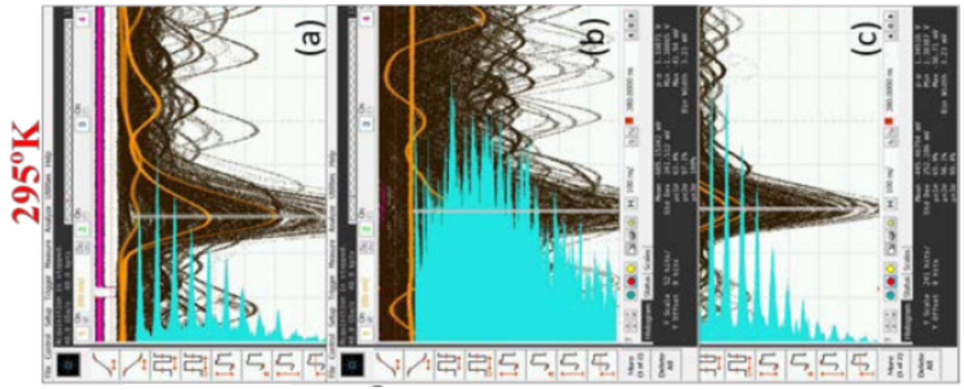

reference

After irradiation
Before annealling

After annealling

T. Tsang, JINST vol11, 2016

X-ray irradiation

δ-ray irradiation

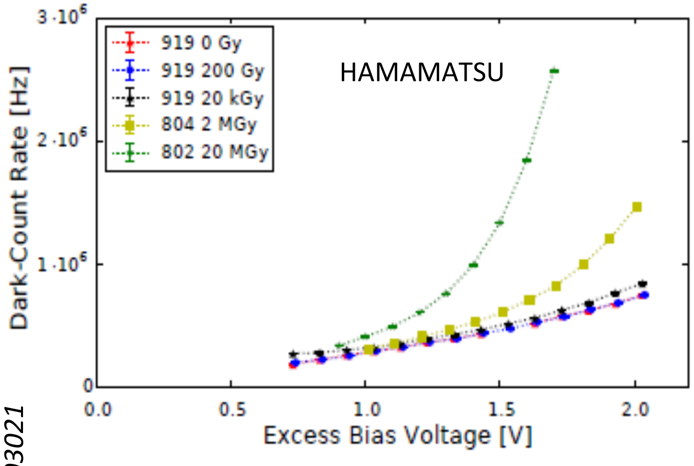

C. Xu, arXiv:1404.3206v2, 2014

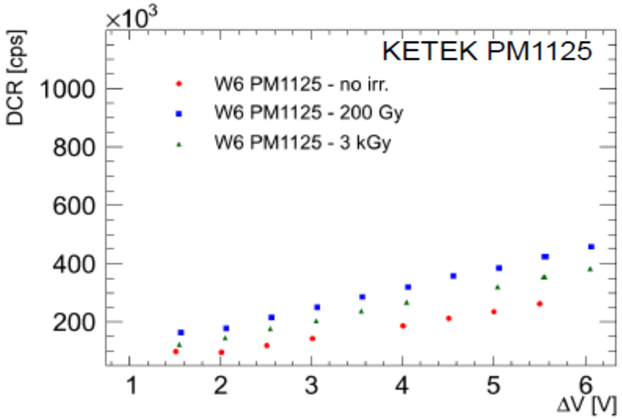

E. Garutti, IPRD13, 2014 JINST 9 C03021

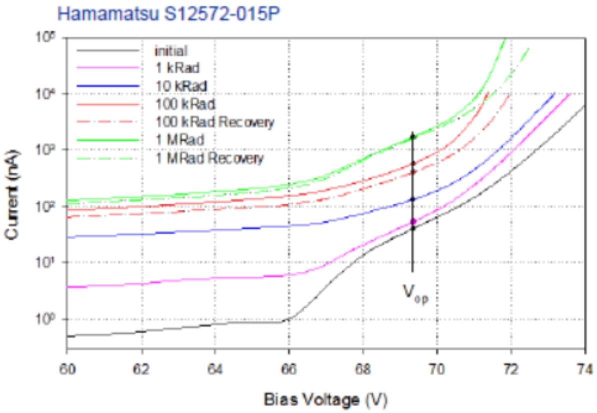

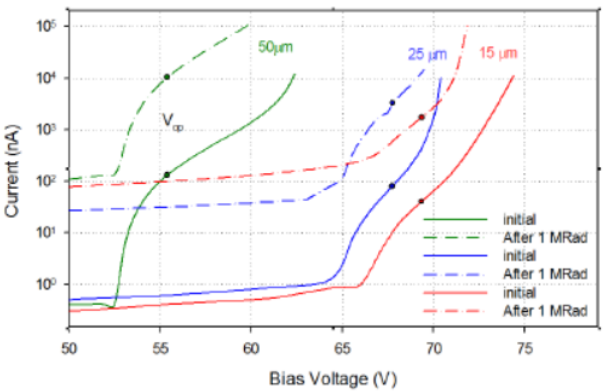

C.Woody, CPAD Workshop 2016

- No significant change in V_{BD}
- Increased of the dark current

- Increased current below V_{BD} may be due to surface current.
- No short term recovery at room temperature.

X and δ produce comparatively lower damage than hadrons

Low radio isotopic SiPM

For rare event search experiment in low background noise, the photodetector is required to suppress radio isotopic(RI) level from its constituent material as far as possible → new MPPC with cryogenically-compatible ultralow RI-level packages

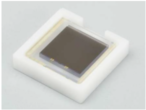

- Package type : Ceramic (active area: 6 mm²)
- Window : bare, quartz (for LXe), MgF_2(for LAr)
- Application : Direct detection of scintillation photons.
- Spectral response range : 120 to 900nm

Unit:[mBq/unit]		MPPC chip	die bonding resin	Pure Ceramic
U-chain	Pa-234m	<99	<211	
	Pb-214	<1.1	<6.8	<65
	Bi-214	<1.7	<13	<105
Th-chain	Ac-228	<3.1	<6.4	<55
	Pb-212	<0.74	<2.1	<35
	Bi-212	<7.6	<89	
	Tl-208	<1.7	<5.6	<60
Other	K-40	<4.7	<22	<220
	Cs-137	<0.33	<2.3	
	Co-60	<0.27	<1.8	<15

HAMAMATSU, private communication

Large SiPMs (4 x 4 – 6 x 6 mm²)

Excelitas C30742-66

HAMAMATSU S10985

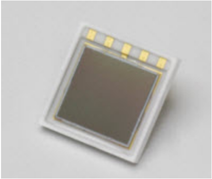

STMicroelectronics

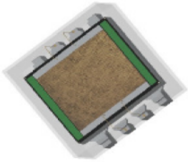

ASD-SiPM4S

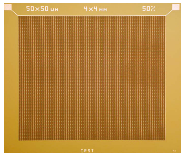

KETEK PM6060

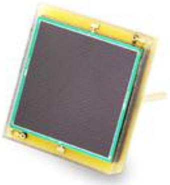

sensL C-series

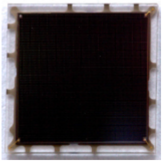

Large areas, high gain, but very high DCR (up to 20 MHz @ room temperature)

Another way to obtain larger area → matrixes

SiPM matrix: packaging and technology

Requirements for the SiPM matrixes:

- improvement of the spatial resolution and PDE
- simplification of the assembly for the building of detectors with large surface and large active area

✓ Discrete array: matrix tileable on almost all their sides but dead space between the channels of the array

✓ Development of monolithic SiPM matrices: all the channels are on the same substrate → small dead spaces, simplification of the assembly but very difficult to produce

✓ Development of discrete array with TSV : no dead spaces

Discrete Array

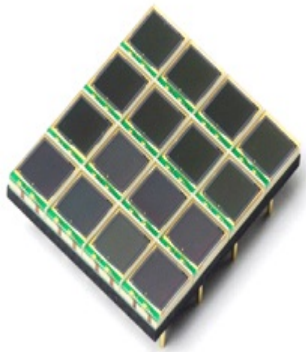

Monolithic Array

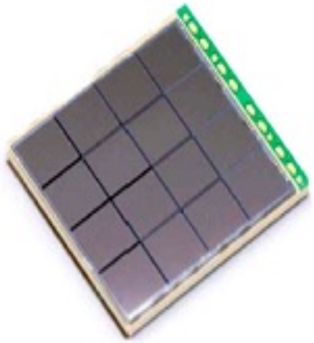

Discrete Array with TSV

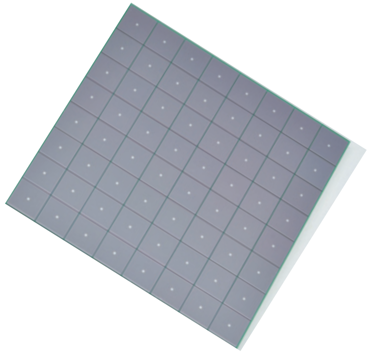

HAMAMATSU development: another way to improve the fill factor and therefore the PDE

Through Silicon Via Technology: each anode is connected by the shortest distance possible to the substrate

with wire bonding (traces to the bonding pads)

with TSV (No traces)

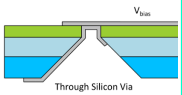

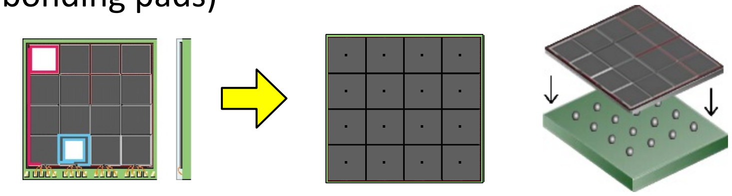

+ high precision assembly → Discrete Array like monolithic array !

S12642-0808PA

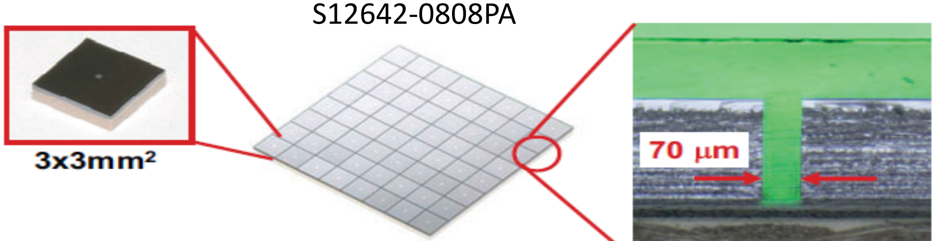

8x8 channels array

16x16 channels array

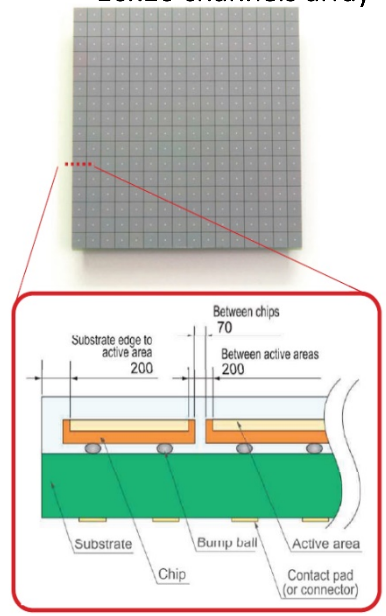

K. Sato, IEEE NSS 2013

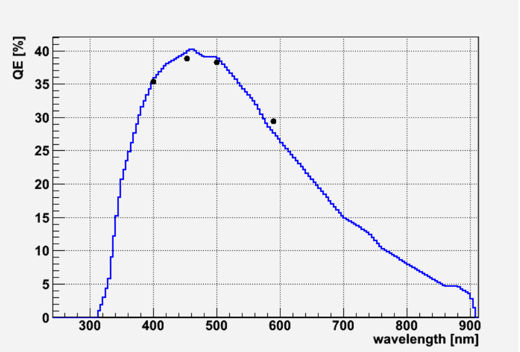

N. Otte, NDIP14

4 sides tileable configuration with very narrow gap between neighboring active areas (200 µm) equivalent to the gap in traditional monolithic type devices

SiPMs matrixes examples

HAMAMATSU

S13361-3050NE-08

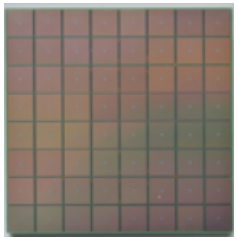

8x8 channels
1 channel= 3 x 3 mm²
3584 cells (50 x 50 µm²) /channel

Ketek

PA3325-WB-0808

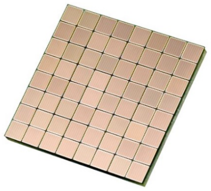

8 x 8 channels
1 channel = 3x3 mm²
15000 cells /channel (25 µm)

Sensl

ArrayJ-60035

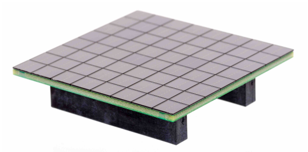

8x8 channels
1 channel= 6 x 6 mm²
20 or 35 µm

AdvansiD

ASD-RGB4S-P-4x4TD

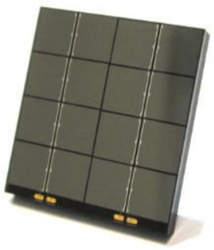

4x4 channels
1 channel = 3x3 mm²
9340 cells (40 x 40 µm²) /channel

Philips Digital Photon Counting

DLS-6400-22-44

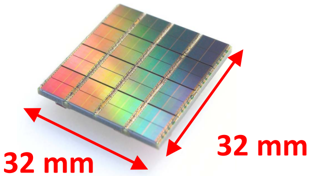

8x8 channels
1 channel = 3.9 x 3.2 mm²
6396 cells (59 x 32 µm²) /channel
Electronics embedded

SiPM applications in HEP and Astrophysics

- Calorimeters : CALICE AHCAL, CMS HCAL upgrade, GlueX, COMPASS II, PANDA,PEBS…
- Cherenkov detectors : IACT (FACT, MAGIC CTA, ASTRI), RICH (Belle II, ALICE), DIRC (PANDA), JEM-EUSO, …
- Neutrino experiments :T2K, NEXT, GERDA, …
- Medical systems : PET, TOF-PET, PET-MRI, dose monitoring, radio-isotopic probes
- Others : nuclear waste storage, volcano studies, ….

some examples →

SiPMs for neutrino oscillation experiment: T2K

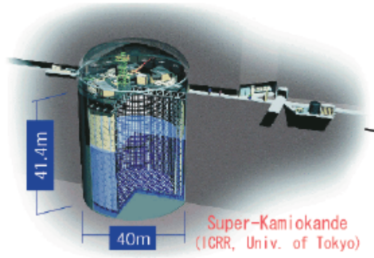

Far detector : Super Kamiokande

ND280 : near detector complex - neutrino beam flux and spectrum measurements

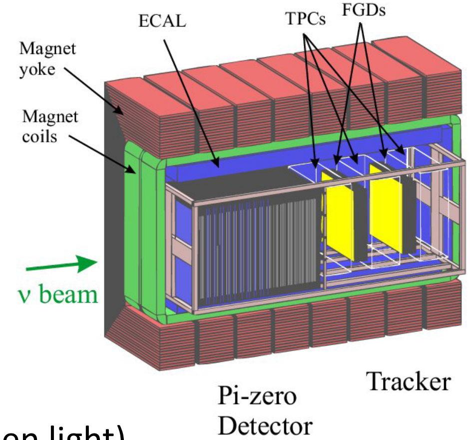

HAMAMATSU MPPC customized device

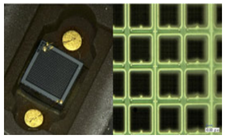

1.3 x 1.3 mm²

667 cells (50 x 50 μm²)

Photodetector requirements:

- insensitive to magnetic field
- coupling with a scintillator + WLS fiber (PDE > 20 % for green light)
- DCR < 1 MHz
- compact

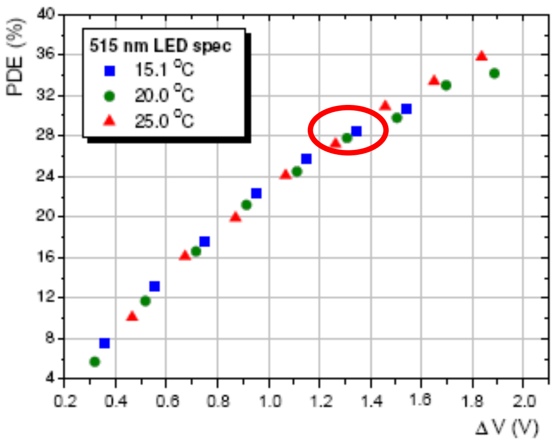

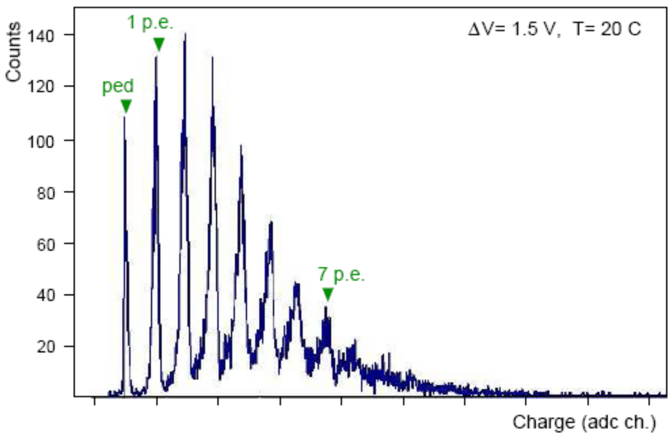

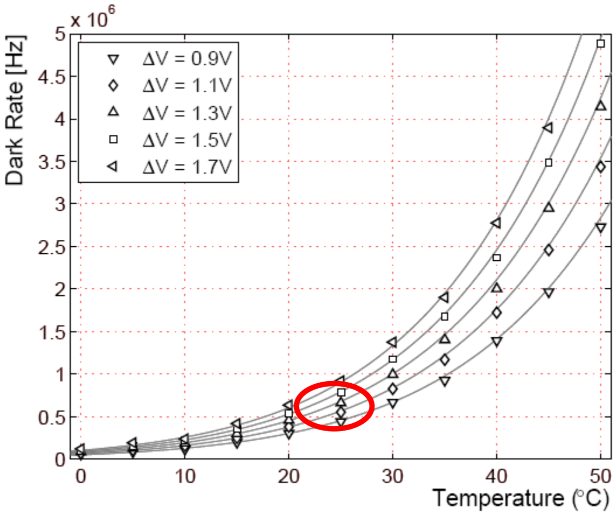

55996 MPPC tested : only 0,16 % rejected

A. Vacheret, arXiv:1101.1996

68

LHCb scintillating fibre tracker

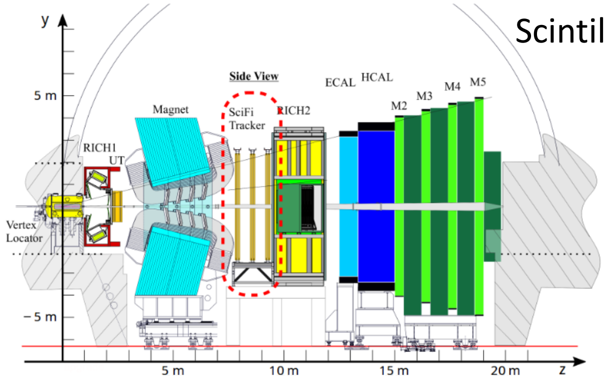

Current tracking detectors downstream of the LHCb dipole magnet will be replaced by the Scintillating Fibre (SciFi) Tracker

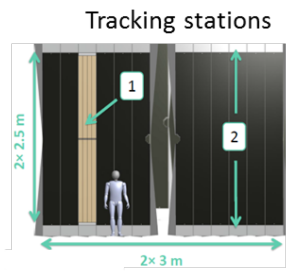

The LHCb SciFi tracker key elements:

- ✓ 11000 km fibres (Ø250 µm)
- ✓ ***4096 SiPM multichannel arrays*** → **590k channels**
- ✓ Operation in radiation environment: 6x10^{11} n/cm² + + 100 Gy ionizing dose → Cooling system for operation of at -40°C

Custom SiPM 128-channel array (Hamamatsu S13552-HRQ)
Channel: 0.250 × 1.625 mm² with 104 pixels
Assembled on a flexible PCB which is pre-shaped to fit in the cooling system

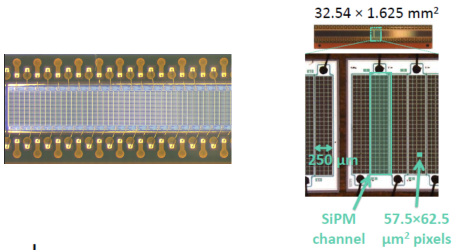

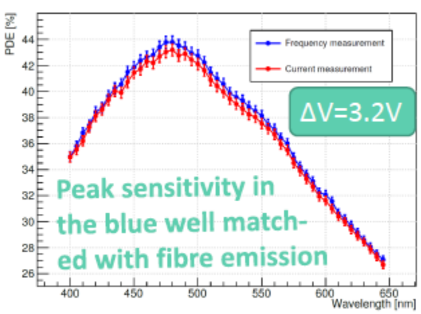

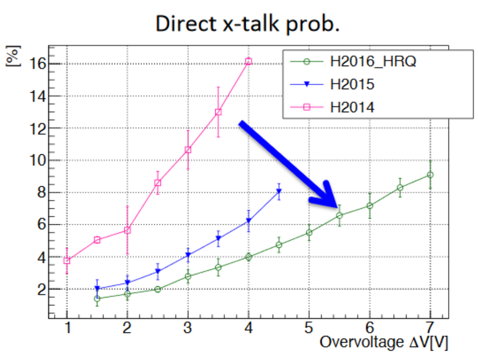

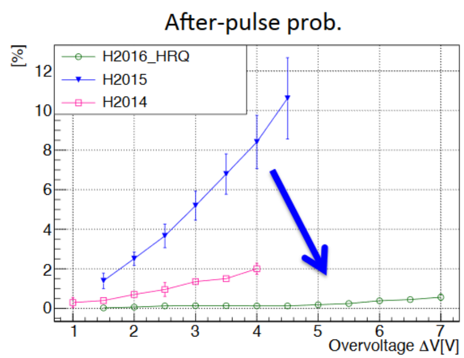

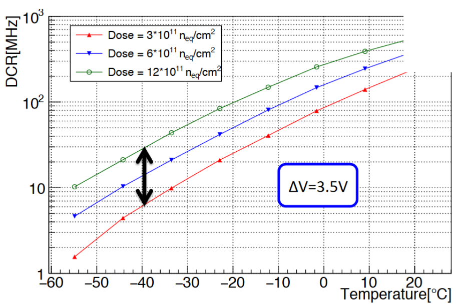

@ ΔV= 3.5V peak PDE = 44% - cross-talk ≈ 3 % - after-pulse = 0.1% - DCR after a dose of 6x10^{11}neq/cm² = 14.3MHz at -40°C and is reduced a factor 2 every 10°C

Sources: A. Kuonen et al, TIPP2017; O. Girard, IEEE NSS 2017

SiPMs for Calorimeters : Upgrade of the CMS HCAL

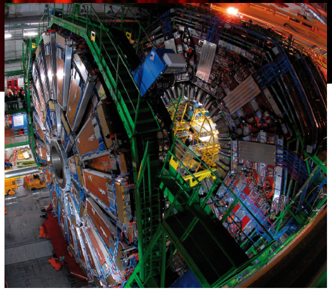

Upgrade Phase 1 : HB & HE upgrade

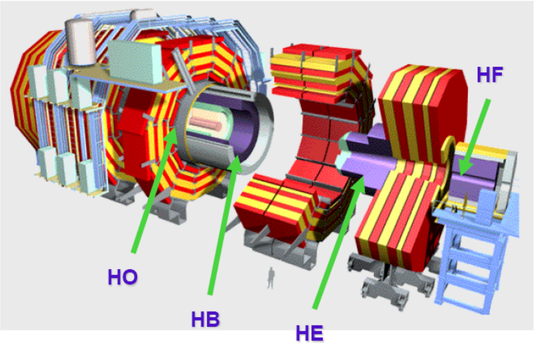

Photodetector requirements (in replacement of the HPD):

- very large dynamic range: a few p.e → 2500 p.e
- high occupancy in front layers in SLHC → fast recovery time (5 – 100 ns)
- radiation hard up to 3.10^{12} 1 MeV neutrons/cm² for 3000 fb^{-1} (Gain*PDE change ≤ 20%)

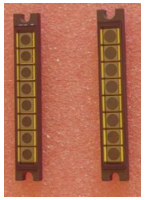

Extensive studies of a large number of SiPM :
HAMAMATSU, ZECOTEK, FBK, CPTA , ST-Micro, Sensl, NDL, KETEK

→ **20 000 large area SiPMs from HAMAMATSU** (2 different areas)

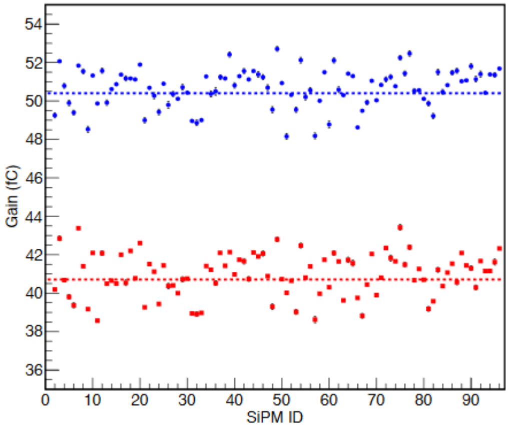

measured gain values for the 50 fC setting (blue) and 40 fC setting (red) for all SiPMs

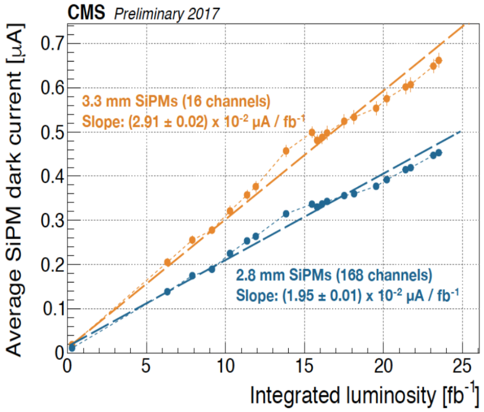

Dark current Increases with integrated luminosity
.

Upgrade Phase 2 : High Granularity Calorimeter to replace the existing endcap calorimeters

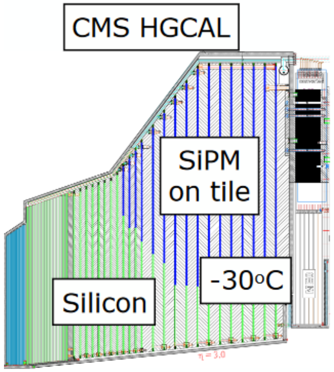

Scintillating tiles with SiPM readout (500000 channels) in low-radiation regions of the HCAL

Sources : S. Chatrchyan et al, 2017 JINST 12 P12034; CMS DP -2017/042

SiPMs for Calorimeters : CALICE AHCAL

High granularity hadronic calorimeter optimised for the Particle Flow measurement of multi-jets final s

Photodetector requirements:

- insensitive to magnetic field (~ 4T)
- good sensitivity in blue-green
- cheap (10 millions channels)

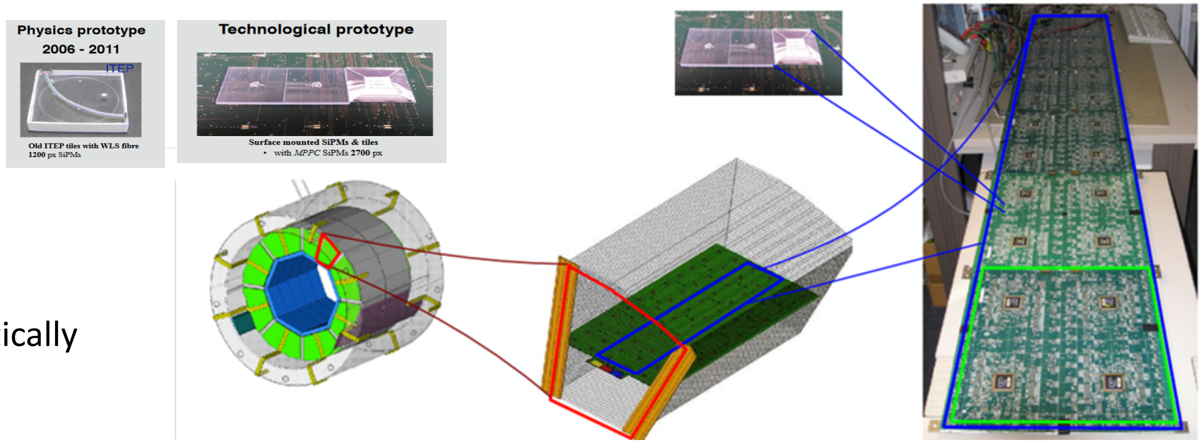

New generation of industrial SiPMs: drastically improved over the past years

- ✓ Dramatically reduced dark rate and increased photon detection efficiency
- ✓ Better signal-to-noise ratio, allows simpler tile design
- ✓ After-pulses and inter-pixel cross-talk largely reduced
- ✓ Noise rate decreases quickly with threshold, much more stable operation
- ✓ Excellent uniformity (operating voltage, gain) → simplified calibration
- ✓ High over-voltage operation → reduced temperature sensitivity

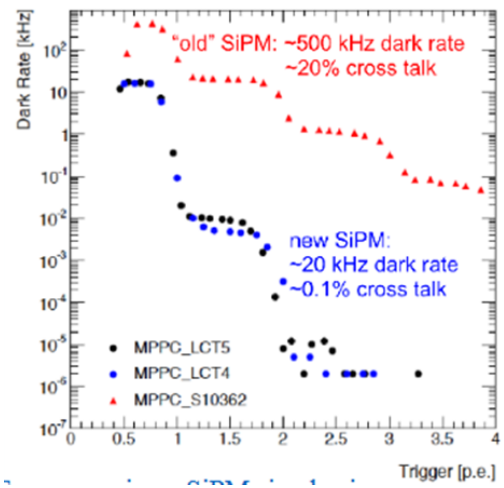

- 24000 MPPC delivered
- Beam test en in 2018

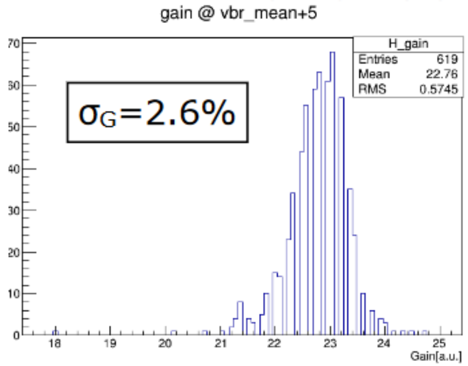

Sources : F. Seskov, CHEF201

SiPMs for Cherenkov Telescope: CTA

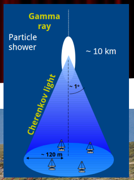

The CTA Consortium is developing the new generation of ground observatories for the detection of ultra-high energy γ rays (100 TeV)

pSCT Telescope

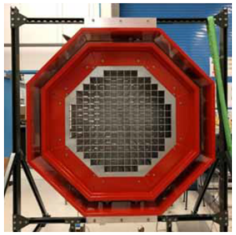

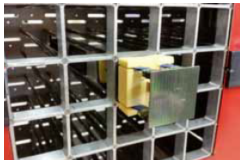

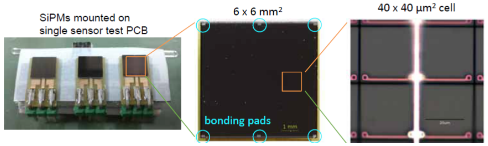

SiPM:

- 1600 NUV-HD devices from FBK
- active area : 0.03 x 6.03 mm²
- PDE > 50 % for NUV light
- fill factor > 80 %

SST-1M Telescope

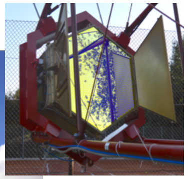

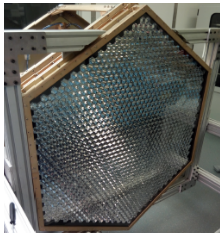

- 1296 hexagonal SiPMs (95 mm ²) from HAMAMATSU
- Entrance window made of borofloat with AR coating (cut at 540nm).
- Water cooling on the aluminium backplate.
- Bias voltage adjusted automatically by a slow control board to compensate for temperature variations.

Showers generated by very high-energy gamma-rays (between a few TeV and 300 TeV) observed in the SST-2M ASTRI camera (May 2017) and the SST-1M (August 2017)

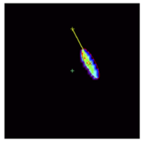

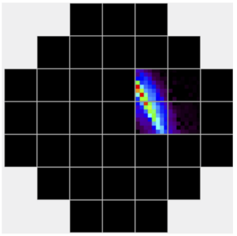

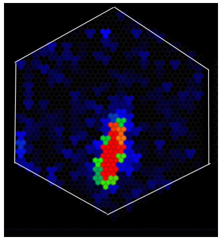

Conclusion

Advantages and drawbacks of SiPMs

		
SiPM	• High gain (10^5-10^6) with low voltage (< 100 V) • Single photo detection • Good timing resolution (SPTR = 40 ps - sigma) • Insensitivity to magnetic field (up to 7 T) • High photon detection efficiency (50 % in blue, > 10 % for VUV) • Large dynamic range (up to 10000 cells/mm²) • DCR ≈ 30 kHz/mm² • Radiation tolerance up to 10^{14} n/cm² • Mechanically robust • A lot of R&D and different producers	• High dark count rate @ room temperature for large device (≥ 9 mm²) • High temperature dependence of the breakdown voltage, the gain • Small devices • Few geometrical configurations available

Documentary sources

Documentary sources and for more explanations

Lectures and Revues :

- **Summer School INFIERI 2013, Oxford***:* Intelligent PMTs versus SiPMs, ***Véronique Puill***
- **IEEE NSS 2016**: Solid State Photo-Detector, ***Gianmaria Collazuol***
- **IEEE NSS 2016:** Recent Progress in Silicon Photomultipliers, ***Yuri Musienko***

Books:

- **Physics of semiconductor devices** – 3rd edition, ***S.M Sze*** (*John Willey & Sons*)

Reference articles:

- **Silicon Photomultiplier - New Era of Photon Detection** from Valeri Saveliev
- **Advances in solid state photon detectors** from D. Renker and E. Lorenz
- **Silicon Photo Multipliers Detectors Operating in Geiger Regime: an Unlimited Device for Future Applications** from G. Barbarino, R. de Asmundis, G.a De Rosa, C. M Mollo, S. Russo and D. Vivolo

Articles and presentations:

All quoted under the figures and plots of this presentation (my apologies if I forgot some of them)